Catalysts **2015**, *5*, 561-594; doi:10.3390/catal5020561

OPEN ACCESS

catalysts

ISSN 2073-4344

www.mdpi.com/journal/catalysts

Review

Deactivation of Pd Catalysts by Water during Low Temperature Methane Oxidation Relevant to Natural Gas Vehicle Converters

Rahman Gholami, Mina Alyani and Kevin J. Smith *

Department of Chemical & Biological Engineering, University of British Columbia, 2360 East Mall, Vancouver, BC V6T 1Z3, Canada; E-Mails: rgshahrestani@chbe.ubc.ca (R.G.); malyani@chbe.ubc.ca (M.A.)

* Author to whom correspondence should be addressed; E-Mail: kjs@mail.ubc.ca; Tel.: +1-604-822-3601; Fax: +1-604-822-6003.

Academic Editor: Calvin H. Bartholomew

Received: 17 December 2013 / Accepted: 25 March 2015 / Published: 31 March 2015

Abstract: Effects of H_2O on the activity and deactivation of Pd catalysts used for the oxidation of unburned CH_4 present in the exhaust gas of natural-gas vehicles (NGVs) are reviewed. CH_4 oxidation in a catalytic converter is limited by low exhaust gas temperatures (500–550 °C) and low concentrations of CH_4 (400–1500 ppmv) that must be reacted in the presence of large quantities of H_2O (10–15%) and CO_2 (15%), under transient exhaust gas flows, temperatures, and compositions. Although Pd catalysts have the highest known activity for CH_4 oxidation, water-induced sintering and reaction inhibition by H_2O deactivate these catalysts. Recent studies have shown the reversible inhibition by H_2O adsorption causes a significant drop in catalyst activity at lower reaction temperatures (below 450 °C), but its effect decreases (water adsorption becomes more reversible) with increasing reaction temperature. Thus above 500 °C H_2O inhibition is negligible, while Pd sintering and occlusion by support species become more important. H_2O inhibition is postulated to occur by either formation of relatively stable $Pd(OH)_2$ and/or partial blocking by OH groups of the O exchange between the support and Pd active sites thereby suppressing catalytic activity. Evidence from FTIR and isotopic labeling favors the latter route. Pd catalyst design, including incorporation of a second noble metal (Rh or Pt) and supports high O mobility (e.g., CeO_2) are known to improve catalyst activity and stability. Kinetic studies of CH_4 oxidation at conditions relevant to natural gas vehicles have

quantified the thermodynamics and kinetics of competitive H_2O adsorption and $Pd(OH)_2$ formation, but none have addressed effects of H_2O on O mobility.

Keywords: natural gas vehicle; exhaust gas; methane; oxidation; catalyst; deactivation; palladium; water

1. Introduction

Natural gas, an abundant energy resource with worldwide proven reserves of over 204.7 trillion m^3 [1], is used primarily for electricity generation and heating. The composition of natural gas (NG) is highly variable, but CH_4 typically accounts for 80–90% of the components of NG. CH_4 has the highest H/C ratio among all hydrocarbon fuels and during combustion, generates the lowest amount of CO_2 per unit of energy. The amount of SO_2 generated during NG combustion is also relatively low because the S content of NG is significantly lower than that of gasoline or diesel fuels. These environmental benefits, together with a relatively low cost of NG, have resulted in an increased interest in its use as a transportation fuel. Currently there are >16 million natural gas vehicles (NGVs) in operation around the world, and their numbers are growing at about 20% annually [2]. However, a significant concern for the wide-spread implementation of NG as a fuel for combustion engines is that unburned CH_4, expelled in the engine exhaust, is a significant greenhouse gas with potency more than 25xs that of CO_2.

The transportation sector is a major contributor to air pollution through the combustion of gasoline and diesel fuels, accounting for ~77% of CO emissions, ~47% of hydrocarbon emissions and ~60% of NO_x emissions in the USA [3]. The exhaust gas of a conventional gasoline powered spark-ignition internal combustion engine (SI-ICE) consists mostly of N_2 (70–75%), CO_2 (11–13%) and water (10-12%) with about 1–2% of pollutants, specifically unburned hydrocarbons, CO and NO_x [4,5]. The pollutants must be removed before the exhaust gas is emitted to the atmosphere so as to meet increasingly stringent worldwide emission standards. The pollutants present in the engine exhaust are dependent on the engine air/fuel (A/F) ratio. For example, if the A/F ratio is above the stoichiometric value for complete combustion (A/F = 14.6), the concentration of reducing agents (hydrocarbons and CO) in the exhaust gas decreases whereas the concentration of oxidizing agents (O_2 and NO_x) increases. Consequently, several different strategies have been developed to control engine emissions, depending on the operating conditions and the target emission levels [5]. Typically, a gasoline engine management system controls the A/F ratio or the exhaust gas composition (using an oxygen sensor connected to a secondary air supply) near the stoichiometric value. A single three-way catalyst (TWC) bed, placed in the exhaust gas flow, ensures simultaneous oxidation of the CO and hydrocarbons and the reduction of the NO_x. Alternatively, dual-bed systems combine a NO_x reduction catalyst bed with a separate oxidation catalyst and secondary air to remove the CO and hydrocarbons. Under lean-burn conditions a gasoline engine may operate with sufficiently high A/F ratios so as to obtain a significant reduction in CO and NO_x emissions and improved fuel efficiency. The function of the catalyst in this case is limited to the oxidation of mainly hydrocarbons, while the NO_x emissions are captured using a NO_x trap followed by desorption and reduction in a TWC during an occasional near stoichiometric

excursion of the engine. Although lean-burn engines improve fuel efficiency, the exhaust gas temperature is significantly lower than from conventional gasoline powered engines, and consequently, catalysts with high oxidation activity at relatively low temperatures are needed for this application [5].

Modern TWC converters used in gasoline ICEs contain Pt, Rh and Pd, dispersed on a washcoat applied to a cordierite ceramic monolith or metal monolith [3,5]. The monolith usually has a honeycomb structure with 1 mm square channels to accommodate the high gas throughputs from the exhaust with minimal pressure drop. The washcoat, a mix of several metal oxides (Al_2O_3, CeO_2, ZrO_2), is applied to increase the metal support surface area (Al_2O_3), to improve thermal stability (ZrO_2) and to provide enhanced oxygen storage capacity (CeO_2) that widens the operating range for optimal oxidation and reduction by the catalyst. The metal composition of the converter varies with application but typically contains 5–20:1 of Pt:Rh with a total metal loading of 0.9–2.2 g L^{-1}. Pd may be used to replace all or part of the Pt for cost savings [5].

Exhaust gas emissions from NGVs are difficult to control because low concentrations of CH_4 (400–1500 ppmv) must be oxidized in the presence of high concentrations of H_2O (10-15 vol.%) and CO_2 (15 vol.%) at relatively low exhaust gas temperatures (450–550 °C). The greater strength of the C-H bond in CH_4 (450 kJ/mol) relative to other hydrocarbons [6] implies that catalysts with high CH_4 oxidation activity must be used. NGVs operate near the stoichiometric point or under lean-burn conditions [7,8]. Stoichiometric NGV engines are primarily used in light-duty passenger cars, whereas lean-burn engines are more common in heavy-duty vehicles such as buses. Over the past ~20 years, conventional converter technologies have been adapted for NGVs using Pd catalysts (which have the highest activity for CH_4 oxidation [7,9,10]) to adequately reduce (by 50–60%) the CH_4 content in NGV exhausts at <500 °C in the presence of high H_2O concentrations. Commercial catalysts for SI-NG engines also typically incorporate a CeO_2/ZrO_2 solid solution for high O_2 adsorption capacity, which serves to buffer O_2 concentration during the rapid switching between slightly oxidizing and reducing conditions close to a stoichiometric mixture (e.g., [7,11]).

Several papers and reviews have assessed the activity and deactivation of Pd catalysts for CH_4 oxidation, supported on Al_2O_3, SiO_2, ZrO_2, CeO_2, and zeolites; promoted with noble metals, e.g., Pt and Rh, and with transition metal oxides, e.g., oxides of Co, Ni, and Sn [6,7,10–20]. Studies have largely focused on CH_4 oxidation on supported Pd catalysts containing 0.5 to 5% Pd (typical Pd loadings in commercial SI-NG monolithic coated catalysts are about 3–7 g.L^{-1}, equivalent to about 1.5–4 wt.% loading in a monolith washcoat) at temperatures ranging from 450 to 600 °C and at CH_4 concentrations of 0.04 to 1 vol.% (0.04 to 0.15 vol.% for commercially representative tests). High activity for CH_4 oxidation appears to be favored by Pd loadings of 3–5 g L^{-1} and dispersions lower than about 0.12–0.15 [7]. Pd-O sites associated with Pd/CeO_2 surfaces appear to have the highest activity for CH_4 oxidation [21,22].

Mechanisms and kinetics of CH_4 oxidation over Pd/PdO catalysts have elicited continued debate in the literature [6,13,14,23], for which data interpretation is complicated by the transitions that Pd catalysts undergo during thermal pre-treatment and reaction [24]. Furthermore, the high concentration of H_2O in the NGV exhaust and the typically transient reaction conditions that result from cycling

between oxidizing and reducing conditions in the NG engine [6,11] are known to significantly impact catalyst activity and stability.

The present review is focused on the inhibition and deactivation effects of H_2O, especially at the relatively low temperatures representative of CH_4 oxidation over Pd catalysts in a NG engine. Although previous reviews have addressed the issue of Pd catalyst stability in the presence or absence of H_2O [4,12,20,25], and several catalyst deactivation mechanisms are possible at the exhaust gas conditions [26], several unresolved issues remain. More recent studies of the past decade have provided new insights into the effects of H_2O, especially at lower temperatures, and these are the focus of the present review. Note, however, that in many cases, fresh catalysts in powder form have been evaluated using ideal fixed-bed micro-reactors and simulated exhaust gas under steady state operating conditions. Tests of monolith catalysts with promoters suitably aged and operated with A/F frequency and amplitude modulation that occur in a vehicle are few [7,11]. Nonetheless, interpretation of data from ideal catalyst studies allows direct links to be drawn between fundamental catalyst properties and catalyst performance for CH_4 oxidation, whereas in real systems this may be more difficult to achieve.

2. Effects of H_2O on CH_4 Oxidation over Pd Catalysts

Water is a major component of the engine exhaust and is also a product of the combustion that occurs in the catalytic converter. In TWCs, H_2O acts as an oxidizing agent for CO conversion by the water-gas-shift reaction and for steam reforming of hydrocarbons [4]. H_2O also significantly affects the thermal stability of the metals (Pt, Rh and Pd) present in the TWC as well as the support, mostly through sintering mechanisms [4,27,28] and by changes in the Pd oxidation state during hydrothermal aging [29]. Water may also act as a reaction inhibitor by adsorption onto the catalyst.

Bounechada *et al.* [11] reported on the activity of a Pd-Rh (Pd/Rh = 39/1) TWC converter supported on stabilized Al_2O_3, promoted with Ce-Zr (Zr/Ce = 3.5) and wash coated on a ceramic honeycomb monolith, tested under fuel-lean ($\lambda > 1$), stoichiometric ($\lambda = 1.00$), and fuel-rich ($\lambda < 1$) conditions (gas composition: 0.15 vol.% CH_4, 0.6% CO, 0.1% H_2, 10% H_2O, 10.7% CO_2, 0.13% NO, 0–1.14% O_2; λ was varied by changing feed O_2 concentration; GHSV = 50,000 h^{-1}). At stationary conditions (constant λ; steady-state experiment), the CH_4 conversion was observed to continuously decrease under both stoichiometric (52 to 43% after 0.5 h reaction) and fuel-lean (from 62 to 59% after 0.5 h reaction) conditions, even though injecting a fuel-rich pulse during fuel-lean stationary operation increased the CH_4 conversion to its initial value at the onset of reaction. The authors attributed the deactivation under fuel-lean conditions to the inhibition effect of H_2O on the CH_4 oxidation reaction, whereas under stoichiometric conditions, partial reduction of PdO due to the lack of oxygen, may lead to a loss in PdO active sites for CH_4 oxidation. The authors also claimed that the presence of high oxygen capacity metals (Ce and Zr) in the catalyst made the reduction of PdO improbable under stoichiometric conditions. Under fuel-rich conditions, H_2O acts as an oxidant through water-gas shift and steam reforming reactions.

2.1. Water Concentration and Reaction Temperature Effects on CH_4 Oxidation Activity of Pd Catalysts

With the growing interest in NGVs, recent studies have focused on effects of H_2O on Pd catalysts during CH_4 combustion [16,18,30–38]. Deactivation or inhibition effects of H_2O are dependent upon several factors including catalyst formulation, reaction temperature, catalyst time-on-stream history, and H_2O concentration. Table 1 summarizes selected data that show effects of H_2O added to the feed gas during CH_4 light-off experiments over Pd catalysts. The light-off temperature (here reported as the temperature corresponding to 30% CH_4 conversion during temperature programmed reaction, T_{30}) increases as the H_2O concentration increases, showing a clear inhibition effect that increases in magnitude with increasing H_2O concentration.

In several cases the effects of H_2O have been examined by measuring the CH_4 conversion at steady-state, with and without H_2O added to the feed gas. A typical set of data, reported by Persson *et al.* [35], is shown in Figure 1 using several Pd/Al_2O_3 catalysts reacted at 500 °C. These data also show that added H_2O significantly suppresses CH_4 conversion, but the effect is at least partially reversible. Similar effects of H_2O addition have been reported in the literature, as summarized in Table 2. These reports confirm that H_2O acts as an inhibitor of CH_4 oxidation over Pd catalysts and that upon removal of the H_2O from the CH_4/O_2 reactant, the inhibition is partially reversible [31,33].

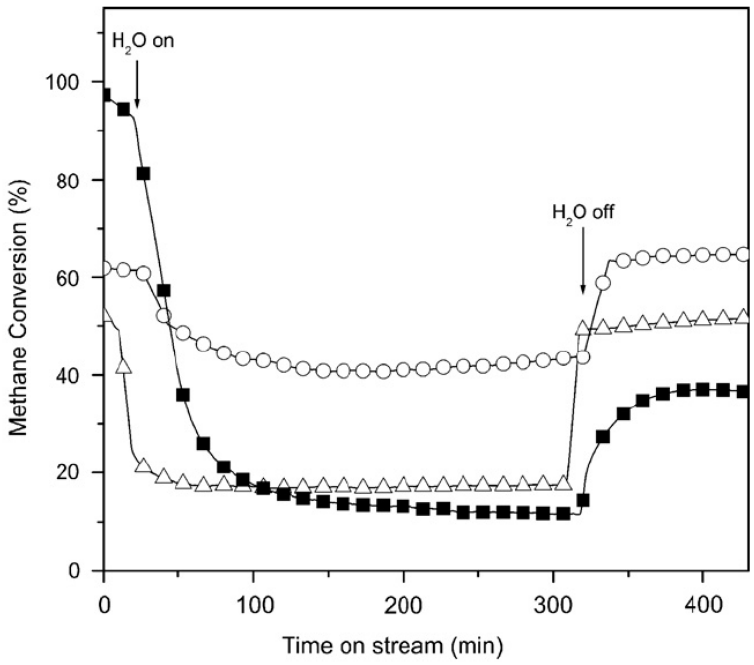

Figure 1. Effect of water vapor on the activity for CH_4 combustion over Pd/Al_2O_3 (■); 2:1 $PdPt/Al_2O_3$ (Δ); and 1:1 $PdPt/Al_2O_3$ (o) at 500 °C; 5 vol.% of steam was added to the 1.5% CH_4/air feed gas, GHSV = 100,000 h^{-1}, for 5 h. [35] Copyright© 2007 Elsevier.

Table 1. Effect of H_2O addition on T_{30} (temperature at 30% CH_4 conversion) during temperature-programmed CH_4 oxidation over Pd catalysts.

	Reference [16]			**Reference [39]**	
	1.1% Pd/Al_2O_3	1.1% Pd/SnO_2	1.1% Pd/Al_2O_3-36NiO	0.9% Pd/ZrO_2 [a]	0.9% Pd/ZrO_2 [b]
GHSV, h^{-1}	48,000			50,000	
Dry feed gas composition, vol.%	1% CH_4/20% O_2 in N_2			0.4% CH_4/0.05% CO/5% CO_2/10% O_2 in N_2	
	T_{30}, °C			T_{30}, °C	
Added H_2O, vol.%					
0	345	290	372	360	300
1	400	315	372	-	-
5	430	335	420	-	-
10	460	360	425	410	350
20	510	365	445	-	-

[a] Calcined at 873K for 6 h; [b] Calcined at 1273 K for 6 h.

Table 2. H_2O inhibition over Pd catalysts during CH_4 oxidation.

Catalyst	**Reaction conditions**			Conc. vol %	Period [a] min	**Water addition** CH_4 Conversion, %			**Comments**	**Refs.**
	Temp °C	**GHSV h^{-1}**	**Feed Gas mol %**			Before H_2O addition	During H_2O addition	After H_2O addition		
0.1 wt.% Pd/H-beta	400	120,000	0.2% CH_4/10%O_2 in N_2	10	100	75	15	58	Conversion after 400 min TOS with periodic water addition	[38]

Table 2. *Cont.*

Catalyst	Reaction conditions			Conc. vol %	Period [a]	Water addition CH_4 Conversion, %			Comments	Refs.
	Temp °C	GHSV h^{-1}	Feed Gas mol %			Before H_2O addition	During H_2O addition	After H_2O addition		
1.3 wt.% Pd/HTNU-10[c]	400	120,000	1% CH_4/4%O_2 in N_2	5	900	43	8	40	Conversion after 35 h TOS with periodic water addition	[33]
5 wt.% Pd/Al_2O_3	500	100,000	1.5% CH_4 in air	5	300	95	13	30	Initial activity	[35]
2 wt.% Pd/Al_2O_3	550	160,000	0.4% CH_4 in air	10	60	95	79	92	Conversion after 400 min TOS with periodic water addition	[32]
1 wt.% Pd/Al_2O_3	600	160,000	0.4% CH_4 in air	8	60	95	90	93	Conversion after 300 min TOS with periodic water addition	[36]

[a] Period: Time length of water addition period. [b] TOS: Time-on-stream. [c] HTNU-10 is the H-form of a medium pore zeolite with Si/Al = 7.1.

Reaction temperature is another key variable affecting the role of H_2O addition. Although the data of Table 2 cannot be compared directly because of the different operating conditions, they do show that at 600 °C, the decrease in CH_4 conversion with H_2O addition is much less significant than at lower temperatures (400 °C). Several authors have proposed that the deactivation is related to the reaction of H_2O with active PdO sites [16,18,31,40,41], $PdO + H_2O \rightarrow Pd(OH)_2$, resulting in the formation of inactive $Pd(OH)_2$, as first proposed by Cullis *et al.* [40]. Burch *et al.* [31] also reported a strong inhibitory effect of water on Pd catalysts up to 450 °C. However, at higher temperatures the negative influence of water on the activity was very small, suggesting that above 450 °C the reverse reaction ($Pd(OH)_2 \rightarrow PdO + H_2O$) occurs. Eriksson *et al.* [41] observed a significant decrease in CH_4 conversion over a much wider range of temperatures (200–800 °C) after adding 18% H_2O to a CH_4/O_2 feed over a Pd/ZrO_2 catalyst, which was likely due to the relatively high H_2O concentration used in this study. Different results were reported by Kikuchi *et al.* [16] when adding 1 vol.% H_2O during CH_4 oxidation over a Pd/Al_2O_3 catalyst, *i.e.*, a decrease in activity was observed up to about 450 °C and no H_2O inhibition was observed at higher temperatures. However, during addition of 20 vol.% H_2O, the inhibiting effect could be observed up to 600 °C, in qualitative agreement with Eriksson *et al.* [41].

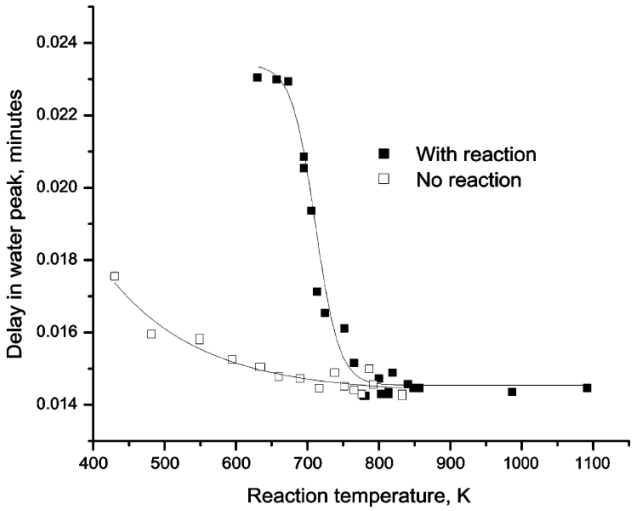

Figure 2. Delay in the H_2O peak with respect to other products obtained by passing pulses of $CH_4/O_2/He$ (closed square) and 1 vol.% O_2/3.45 vol.% H_2O/He (open square) over Pd/ZrO_2 at different temperatures. Reproduced with permission from [42]. Copyright © 2001 Elsevier.

Further insight into the H_2O adsorption/desorption phenomena on Pd/ZrO_2 catalysts has been obtained using pulsed-flow experiments [42,43]. Accordingly, pulses of $CH_4/O_2/He$ (1:4:95 vol %) were passed over a Pd/ZrO_2 catalyst at various temperatures and the products monitored by mass spectrometer. The time at which the peak maximum for H_2O appeared in each spectrum, compared to other products, was reported as the delay in the H_2O peak. The data (Figure 2) show that the H_2O generated during CH_4 oxidation lags other products, suggesting a slow H_2O adsorption/desorption equilibrium which might include spillover to the support. As the temperature increases above 450 °C (723 K), the desorption rate of H_2O increases and the delay in the H_2O peak compared to the other products is insignificant. This behavior is in agreement with observations from other studies [30,31,44]

that the desorption rate of H_2O produced during CH_4 oxidation is slow and on the order of seconds below 450 °C, even though CO_2, the other product of reaction, desorbs very quickly. Increasing temperature above 450 °C removes the desorption time gap between CO_2 and H_2O, and thus, no inhibition by H_2O occurs. Ciuparu *et al.* [42] also pulsed gas containing 3.45 vol.% H_2O/O_2/He but no CH_4 (and hence no reaction) through the same catalyst bed (Figure 2), showing that the H_2O generated from CH_4 oxidation lags the H_2O added to the feed. These data demonstrate that the adsorption/desorption of H_2O from the Pd catalyst surface is temperature dependent and reaches equilibrium at temperatures above ~450 °C (723 K), even for H_2O added in the gas phase.

Figure 3 compares temperature-programmed-reaction (TPR) profiles for CH_4 oxidation obtained over a Pd/ZrO_2 catalyst, from both pulsed and continuous flow experiments with or without H_2O added [42,43]. The pulsed flow TPR profile was obtained by injecting pulses of the reaction mixture (1/4/95:CH_4/O_2/He for the "dry" feed and 1/4/95:CH_4/O_2/He saturated with ~2% H_2O for the "wet" feed) into a He stream every 3 min while ramping the temperature at 0.5 K min^{-1}. Between consecutive pulses the catalyst was purged in flowing He. The pulsed flow data of Figure 3 show that at temperatures above 450 °C (723 K), there is no H_2O inhibition, since the conversions of "dry" and "wet" reaction mixtures are essentially the same. At <450 °C, inhibition is observed due to a low H_2O desorption rate. When H_2O is added to the gas phase, the H_2O adsorption rate is enhanced and the rate of desorption is further decreased. With continuous flow of reactants and a higher H_2O concentration, H_2O inhibition occurs at high temperatures due to re-adsorption. The addition of H_2O to the feed directs the equilibrium towards more H_2O adsorption on the surface and hence a greater decrease in catalyst activity during CH_4 oxidation.

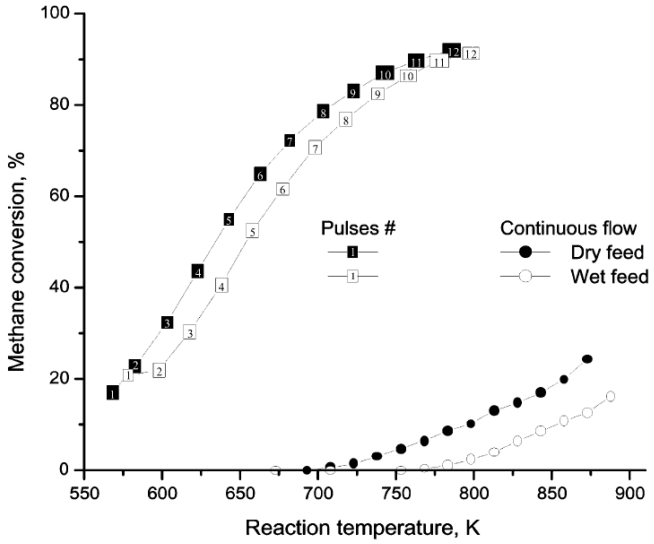

Figure 3. Temperature-programmed reactions during pulsed or continuous flow of reactants over Pd/ZrO_2 with or without H_2O in the feed. Reproduced with permission from [42]. Copyright © 2001 Elsevier.

The above observations are consistent with the following hypotheses: (1) product inhibition of CH_4 oxidation by H_2O on PdO catalysts occurs at temperatures below 450 °C; (2) product inhibition by H_2O is enhanced by its slow rate of desorption from the PdO catalyst relative to a higher rate of CH_4

oxidation; (3) PdO and H_2O may interact via the reversible reaction: $PdO + H_2O \leftrightarrow Pd(OH)_2$ yielding inactive $Pd(OH)_2$ and thus reversibly deactivating PdO as first proposed by Cullis *et al.* [40]; and (4) the extent of the CH_4 oxidation reaction increases with increasing temperature but is reduced with increasing H_2O concentration in the gas phase.

2.2. Catalyst Sintering by H_2O

The possibility that addition of H_2O may degrade Pd catalysts through a sintering mechanism [26] has also been investigated. According to Hansen *et al.* [45], the sintering rate of metal nanoparticles depends on their size. For nanoparticles <3 nm in diameter, Ostwald ripening is the most likely sintering mechanism. For larger particles (3–10 nm), both Ostwald ripening and particle migration and coalescence may occur, but the sintering rate is much slower than for the smaller particles [45]. The particle sintering rate has also been shown to correlate with the vapor pressure of the surface species [4]. Pd is unique among the PGMs in that the oxide (PdO) has a much lower vapor pressure than the metal (Pd), and consequently, one would expect a very low sintering rate of PdO by Ostwald ripening [4]. The rate of sintering is also dependent on the support. Lamber *et al.* [46] suggested that on SiO_2 in the presence of H_2O, the formation of silanol (Si-OH) groups favors the migration and coalescence of Pd, whereas in the absence of H_2O, Ostwald ripening is favored. Sintering suppression has been demonstrated for Pt catalysts using supports that enhance metal-support interactions [28]. Nagai *et al.* [47] demonstrated a correlation between the O electron density of the support, the strength of the Pt-O interaction and the resulting crystallite size. Thus, supports with a stronger metal-support interaction have a higher O electron density and yield smaller Pt crystallites in the order $SiO_2 < Al_2O_3 < ZrO_2 < TiO_2 < CeO_2$ [28,47].

Xu *et al.* [48] reported that the main deactivation mechanism of Pd/Al_2O_3 catalysts following exposure to 10 (*v*/*v*)% H_2O/N_2 at 900 °C for up to 200 h is Pd sintering. A substantial decrease in Pd dispersion from 3.7% to 0.9% over 7 wt.% Pd/Al_2O_3 and similar decreases at other Pd loadings after 96 h hydrothermal aging, were observed. As noted by Xu *et al.* [48], aging the catalyst at 900 °C ensures that PdO decomposition to Pd^0 is complete and consequently the more rapid sintering observed is relevant to the behavior of Pd^0 rather than PdO.

Escandon *et al.* [49] examined effects of hydrothermal aging at lower temperatures, where PdO is thermodynamically stable [6]. A 1 wt.% Pd/ZrO_2-Ce catalyst was hydrothermally aged at 300, 425, and 550 °C in 2% H_2O/Air for 30 h, before being evaluated for CH_4 oxidation under lean-burn conditions (5000 ppmv CH_4 in dry air). The results, shown in Figure 4, are compared with the same catalyst, thermally aged at 550 °C in dry air for 30 h (identified as Pd/ZrO_2-Ce-550 in Figure 4) [49]. A significant irreversible decrease in CH_4 conversion occurs and the extent of catalyst deactivation increases with aging temperature (Figure 4). The $T_{50\%}$ increases from 375 °C for the fresh oxidized catalyst (identified as Pd/ZrO_2-Ce in Figure 4), to 450 °C for the air-aged catalyst and to > 550 °C for the hydrothermally aged catalyst. Pd dispersion and BET surface area of the aged catalysts did not change [49]. Comparing the activity results of the catalyst thermally aged in air (Pd/ZrO_2-Ce-550) with that aged in 2% H_2O/air at 550 °C (Pd/ZrO_2-Ce-550h), confirms that catalyst deactivation rate increases in the presence of H_2O. The stability of the hydrothermally aged catalysts during reaction was also evaluated, using both isothermal deactivation experiments at 500 °C and light-off measurements made after 50 h reaction with 5000 ppmv CH_4 in air. The catalysts aged in the presence

of H_2O at 300 °C underwent a significant deactivation whereas the catalyst aged in the presence of H_2O at 425 °C was much more resistant to deactivation, and after 25 h time-on-stream was the most active of all the catalysts examined. XRD analysis of the catalysts showed that the more stable catalysts are associated with the most stable supports [49].

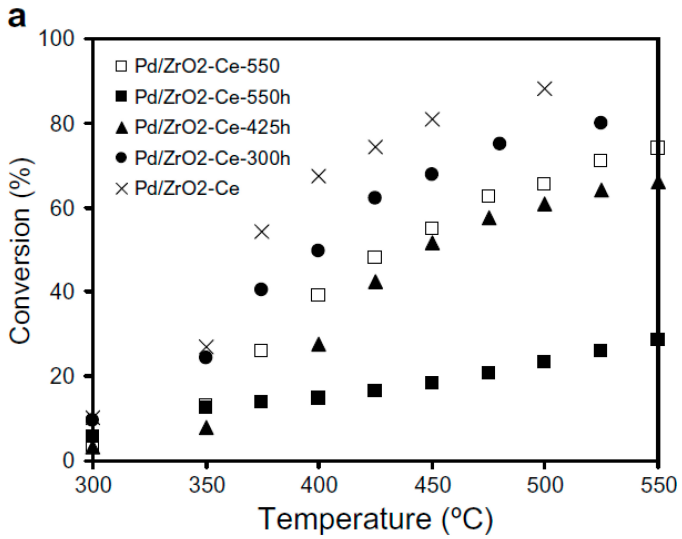

Figure 4. CH_4 conversion over fresh 1 wt.% Pd/ZrO_2-Ce catalyst compared to 1 wt.% Pd/ZrO_2-Ce thermally aged in air at 550 °C (Pd/ZrO_2-Ce-550) and hydrothermally aged at different temperatures in 2% H_2O/air (identified as Pd/ZrO_2-Ce-TTTh where TTT is the aging temperature in °C). Reproduced with permission from [49]. Copyright© 2008 Elsevier.

In another study of CH_4 oxidation at low temperature (250–450 °C), a change in PdO dispersion was suggested as the main cause of deactivation of 0.5% Pd/Al_2O_3 and 0.5% Pd/SiO_2 catalysts [50]. Dispersion decreased from 10% for the unused 0.5% Pd/SiO_2 catalyst to 5.6% for the catalyst reacted in 1% CH_4/air feed at 450 °C for 7 h, whereas for the 0.5% Pd/Al_2O_3 catalyst the corresponding changes in dispersion were 67% to 6.3%, respectively. These observations are in good agreement with that of Narui *et al.* [51], in which the PdO dispersion of a 0.5% Pd/Al_2O_3 catalyst decreased from 14% to 11% after 6 h reaction at 350 °C. Zhang *et al.* [52] investigated Pd catalysts supported on ZSM-5 and reported that catalyst stability is improved when CH_4 oxidation is carried out in the presence of H_2O at 430–480 °C, compared to the reaction in a dry feed. In both cases, the loss in catalyst activity could be related to reduced PdO dispersion, as determined by the Pd/Si ratio measured by XPS, but the loss in dispersion is smaller in the presence of H_2O [52]. By contrast, Araya *et al.* [53] reported an insignificant drop in PdO dispersion (from 31.7% to 28.2%) of a Pd/SiO_2 catalyst after 96 h of reaction at 325 °C in 1.5% CH_4/6% O_2 in He, despite a significant decrease in CH_4 conversion from 32% to 22%. The extent of catalyst deactivation was found to further increase in the presence of 3% H_2O added to the feed.

Several studies have demonstrated that catalyst sintering can be reduced by encapsulating Pd/PdO nanoparticles in support materials. Sinter-resistant Pd catalysts have been prepared by atomic layer deposition of Al_2O_3 overlayers on Pd [54], as well as by the synthesis of Pd/SiO_2 core-shell structures [55,56]. Cargnello *et al.* [22] reported a Pd/CeO_2 core-shell catalyst supported on Al_2O_3 for CH_4 oxidation that is about 200xs more active than an equivalent Pd-CeO_2/Al_2O_3 catalyst prepared by

wet impregnation. The authors demonstrated that the Pd cores remain isolated even after heating the catalyst to 850 °C and that the CH_4 light-off curves (measured at GHSV of 200,000 h^{-1} in a feed gas of 0.5% CH_4, 2% O_2 in Ar) are the same for the fresh catalyst and one that has been aged at 850 °C for 12 hours. The Pd nanoparticles encapsulated by CeO_2 enhance the metal-support interaction that leads to exceptionally high CH_4 oxidation activity and good thermal stability [22].

2.3. Effects of Support

The data of Table 1 show that the inhibition of CH_4 oxidation by H_2O on Pd catalysts is dependent upon the support. Pd/Al_2O_3 shows significantly more inhibition with 10% H_2O added to the feed than either the Pd/SnO_2 or Pd/ZrO_2 catalysts. More detailed data from Kikuchi *et al.* [16] comparing CH_4 light-off curves for a 1.1 wt.% Pd/Al_2O_3 catalyst and a 1.1 wt.% Pd/SnO_2 catalyst with H_2O added to the feed over a range of concentrations (1–20 vol.%), are shown in Figures 5 and 6. By increasing the H_2O concentration, the CH_4 light-off curves for both catalysts shift to higher temperatures. However, the temperature shift is larger over the Pd/Al_2O_3 catalyst than the Pd/SnO_2. The authors completed a simplified kinetic analysis of the CH_4 oxidation rate data to show that the enthalpy of adsorption of H_2O is strongest on the Pd/Al_2O_3 catalyst ($\Delta H_{ad} \sim -49$ kJ/mol), from which they concluded that the significant loss in activity of the Pd/Al_2O_3 in the presence of H_2O is due to a high coverage of the active sites by H_2O [16]. These results could also be interpreted according to the more recent proposals by Schwartz *et al.* [44,57], that hydroxyl accumulation on the support hinders oxygen migration and exchange, and hence CH_4 oxidation. The strong adsorption of H_2O determined by kinetic analysis on the Pd/Al_2O_3 catalyst [16] is consistent with a large hydroxyl accumulation on the catalyst surface that could inhibit the O exchange.

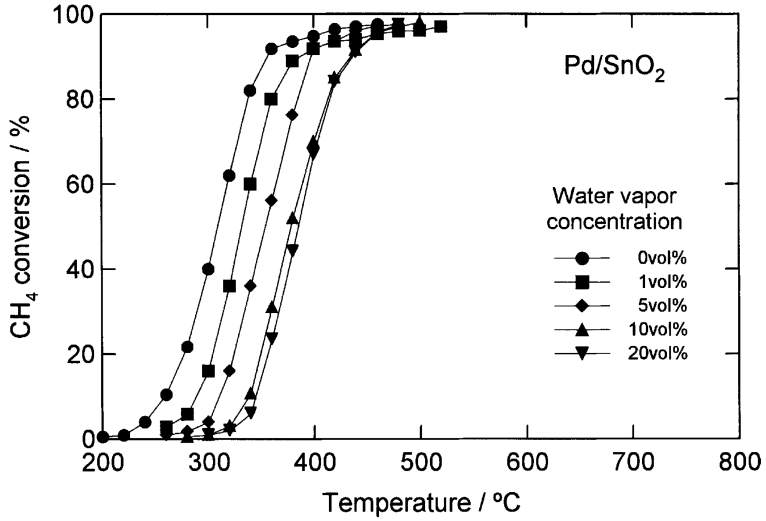

Figure 5. Catalytic combustion of CH_4 over 1.1 wt.% Pd/SnO_2 with different amounts of water added (vol.%). Reaction conditions: CH_4, 1 vol.%; O_2, 20 vol.%; H_2O, 0–20 vol.%; N_2, balance; GHSV 48,000 h^{-1}. Reprinted with permission from [16]. Copyright© 2002 Elsevier.

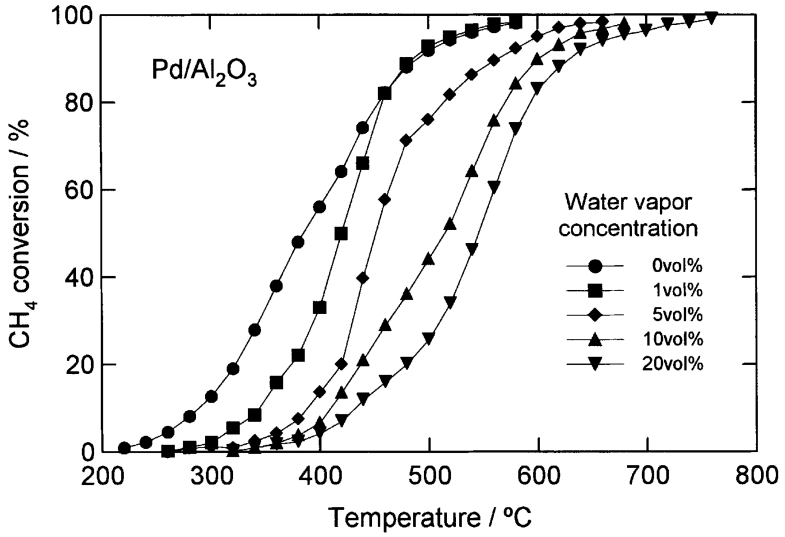

Figure 6. Catalytic combustion of CH_4 over 1.1 wt.% Pd/Al_2O_3 with different amounts of water added (vol.%). Reaction conditions: CH_4, 1 vol.%; O_2, 20 vol.%; H_2O, 0–20 vol.%; N_2, balance; GHSV 48,000 h^{-1}. Reprinted with permission from [16]. Copyright © 2002 Elsevier.

The rate of deactivation during CH_4 oxidation in the presence of H_2O has been shown to be reduced by using a support with high oxygen surface mobility. At temperatures below 450 °C, Ciuparu *et al.* [30] reported the inhibition effect of H_2O to be dependent upon the oxygen mobility of the support. Comparing PdO supported on oxides with increasing surface oxygen mobility: Al_2O_3 < ZrO_2 < $Ce_{0.1}Zr_{0.9}O_2$, they show that the resistance to H_2O inhibition during CH_4 oxidation increases in the same order. The deactivation rate of PdO was also compared over Al_2O_3, MgO, and TiO_2 supports by Schwartz *et al.* [44,57] at temperatures <450 °C. Deactivation is shown to be a consequence of reduced oxygen mobility due to hydroxyl adsorption. They also reported that PdO/MgO catalyst has a slower deactivation rate compared with Al_2O_3 and TiO_2 supports because of the higher oxygen surface mobility on the MgO [44,57]. However, Pd catalysts dispersed on other supports such as MCM-41, which have high surface area (1113 m^2/g) and lower oxygen mobility than MgO and Al_2O_3, did not deactivate either, suggesting that other factors also play a role, depending on the catalyst and the support.

Another study compared the stability of Pd/SiO_2 and Pd/ZrO_2 during CH_4 oxidation using a dry feed gas [53]. The data (Figure 7) show that the Pd/ZrO_2 is stable after 40 h time-on-stream, while the CH_4 conversion over the Pd/SiO_2 catalyst increases from 13% to 32% in the first 3 h, and then decreases to 22% after 96 h (see Figure 7). Although the Pd/ZrO_2 catalyst is more stable than the Pd/SiO_2 catalyst, its conversion is lower than for the Pd/SiO_2 catalyst. The lower deactivation rate observed on the Pd/ZrO_2 is consistent with the higher oxygen mobility of this catalyst compared to Pd/SiO_2, as noted above.

Metal-support interactions, support stability and the tendency of the support to encapsulate Pd, may also play a role in the deactivation of Pd catalysts during CH_4 oxidation. Gannouni *et al.* [58] compared Pd catalysts supported on silica and mesoporous aluminosilicas and showed that, according to the light-off curves measured with 1% CH_4, 4% O_2 in He, CH_4 oxidation activity is enhanced on the pure silica support, whereas on the aluminosilica, the beneficial effect of Al^{3+} on metal dispersion and catalytic activity is counterbalanced by partial metal encapsulation. Above 500 °C in the presence of H_2O, the structural collapse of the support, metal sintering, and metal encapsulation by the support all

occur [58]. Similar effects were reported with SiO_2 supports by Zhu *et al.* [59]. SiO_2 desorbs chemisorbed H_2O (silanol groups –Si-OH) at ~397 °C [46] and the formation of hydroxides according to the reaction: $SiO_{2\,(s)} + 2H_2O_{(g)} \leftrightarrow Si(OH)_{4\,(g)}$ is feasible at temperatures above 700 °C [60,61]. Hydroxyl mobility can change the extent of metal-support interactions [45,46]. Zhu *et al.* [59] reported the encapsulation of PdO by SiO_2 during CH_4 oxidation at only 325 °C. The authors suggested that silica migration by (i) formation of a palladium silicide during H_2 reduction at 650 °C that is subsequently oxidized during CH_4 oxidation and (ii) migration of SiO_2 during CH_4 oxidation caused by the water formed during reaction, are important related factors facilitating the encapsulation of PdO by the SiO_2. Migration of SiO_2 onto the metal crystallites in other catalyst systems containing H_2O has also been reported in the literature [46,62].

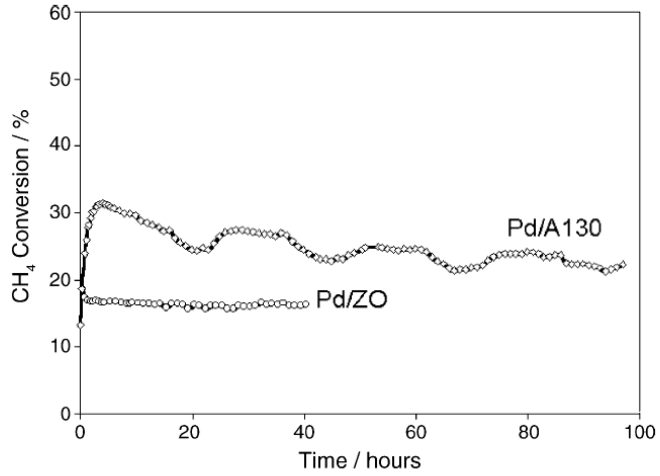

Figure 7. Methane conversion over time of Pd/ZrO_2 and Pd/Aerosil130 catalysts. Reaction conditions: 1.5% CH_4; 6% O_2; total flow = 90 cm^3min^{-1}, balanced in He; temperature = 325 °C; catalyst mass = 0.2 g. Reprinted with permission from [53]. Copyright © 2005 Elsevier.

Yoshida *et al.* [63] also examined the effects of various metal oxide supports of Pd on the low temperature oxidation of CH_4 as summarized in Table 3. The catalytic activity varies with the support, but the support oxides with moderate acid strength (Al_2O_3 and SiO_2) give maximum CH_4 conversion. For these catalysts higher activity corresponds to a higher oxidation state of Pd (bulk PdO). The lower activity of Pd on basic supports is attributed to the formation of binary oxides from PdO and the support (such as Pd/MgO_x), in spite of a high Pd oxidation state.

The effect of metal oxides added to Pd/Al_2O_3 to improve the hydrothermal stability has been reported by Liu *et al.* [36] who showed in particular, that the addition of NiO or MgO improved the hydrothermal stability of Pd/Al_2O_3 through the formation of $NiAl_2O_4$ and $MgAl_3O_4$ spinel structures. According to the authors, the spinel results in weakened support acidity that suppresses the formation of $Pd(OH)_2$ during hydrothermal aging.

Table 3. Effect of support on properties of 5 wt.% Pd catalysts and their CH_4 oxidation conversion. Data adapted from [63].

Support	Support Acid Strength	Pd Dispersion		CH_4 conversion [a], %
	(H_o)	Fresh	Used	
MgO	22.3	0.21	0.20	12
ZrO_2	9.3	0.41	0.12	3
Al_2O_3	3.3	0.35	0.20	59
SiO_2	-5.6	0.09	0.11	58
SiO_2-ZrO_2	-8.2	0.16	0.13	20
SiO_2-Al_2O_3	-11.9	0.12	0.06	10
SO_4^{2-}-ZrO_2	-13.6	-	0.02	11

[a] measured at 350 °C in 0.25% CH_4/3%O_2 in He at GHSV of 1,200,000 h^{-1}.

A comparison of initial CH_4 oxidation activity as a function of temperature for Pd-Pt catalysts on Al_2O_3, ZrO_2, $LaMnAl_{11}O_{19}$, Ce-ZrO_2, and Y-ZrO_2 was reported by Persson *et al.* [64]. Monolith catalysts were tested in a tubular quartz flow reactor at atmospheric pressure in 1.5 vol.% CH_4 in dry air and at a space velocity of 250,000 h^{-1}. In steady-state experiments, reaction temperature was set initially at 470 °C and then increased to 720 °C stepwise in 50 °C increments, with 1-h holds at each temperature. The Pd-Pt/Al_2O_3 catalyst had the highest activity at lower temperatures (470–570 °C), while the Pd-Pt/Ce-ZrO_2 catalyst had the highest activity between 620 °C and 800 °C [64]. The authors suggested that the higher surface area of the Al_2O_3 compared to the other supports (e.g., 90 m^2/g for Al_2O_3 *versus* 10 m^2/g for Ce-ZrO_2) accounts for the higher activity of Pd-Pt/Al_2O_3 at lower temperatures, due to higher dispersion of Pd-Pt oxides, while at higher reaction temperatures the Pd-Pt catalyst probably undergoes reduction to the metal. A combination of lower activity for Pd metal and its propensity for rapid sintering probably explain the lower activity. The authors also suggested that the Ce-ZrO_2 likely enhances the stability of the PdO, similar to the enhanced stability observed on CeO_2 [30]. In addition, ZrO_2 has high oxygen mobility [30] and the ability to re-oxidize metallic Pd into PdO should be higher. Indeed, Pd/alumina is re-oxidized very slowly, whereas Pd supported on ceria-stabilized ZrO_2, is re-oxidized more rapidly.

Since H_2O adsorption on the Pd and/or the support is an important step in inhibiting CH_4 oxidation over Pd, support hydrophobicity may be expected to impact the inhibition effect of H_2O. Araya *et al.* [53] studied this effect on the deactivation of Pd-based catalysts by preparing 1 wt.% Pd on two different commercial silicas, Aerosil130 and Aerosil R972. The Aerosil R972 is hydrophobic since the OH groups have been replaced by methyl groups. Both 1% Pd/A130 and 1% Pd/R972 were tested at 325 °C in a gaseous mixture of 1.5% CH_4 and 6% O_2 in He at a total flow rate of 90 cm^3 min^{-1} with addition of 3% H_2O after 2 h As shown in Figure 8, the effect of H_2O addition to the feed gas is

approximately the same for the hydrophobic silica, Pd/R972, and the hydrophilic Pd/A130. In both cases, a large decrease in CH_4 conversion is observed with the introduction of H_2O to the reactor. The authors reported a reaction order with respect to H_2O of −0.25 for both Pd/A130 and Pd/R972, emphasizing that the hydrophobicity of the support does not affect the extent of H_2O inhibition observed on either catalyst.

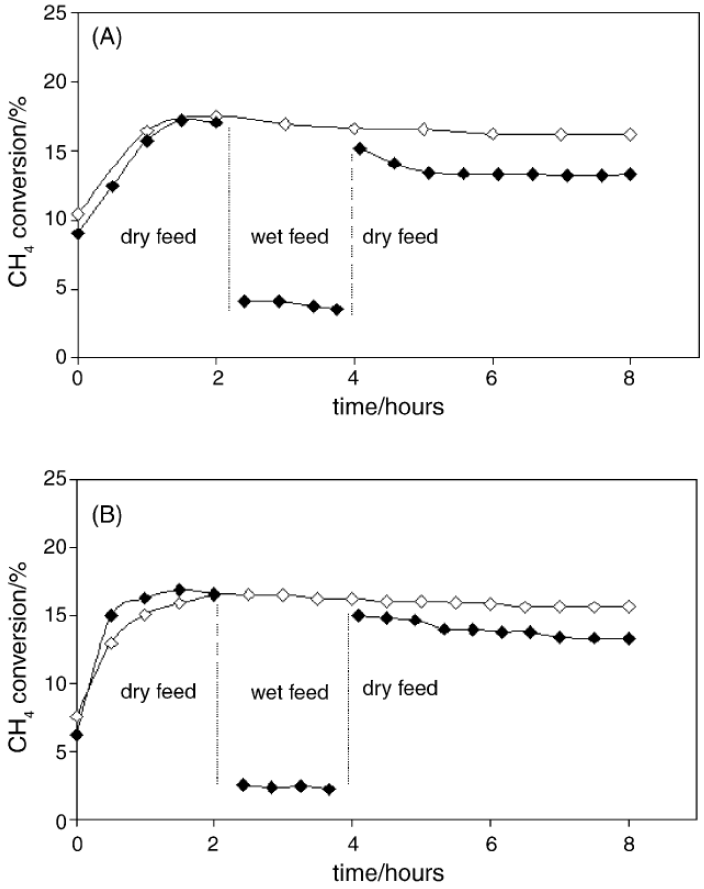

Figure 8. (A) Pd/Aerosil130 catalyst, **(B)** Pd/R972 catalyst. Reaction conditions: total flow = 90 cm^3 (STP) min^{-1}, temperature = 325 °C; catalyst mass = 0.2 g. Open symbols: dry feed 1.5% CH_4; 6% O_2;balance He; closed symbol: wet feed 1.5% CH_4; 6% O_2 with 3% H_2O, balance He. Reproduced with permission from [53]. Copyright © 2005 Elsevier.

2.4. H_2O Inhibition and Hydroxyl Formation

Although $Pd(OH)_2$ has been postulated as a cause for deactivation of PdO catalysts in the presence of H_2O [18,31,32,40], and while this mechanism is consistent with many of the observations discussed above, recent evidence obtained from FTIR and isotopic labeling experiments that monitor the formation and conversion of hydroxyls on the catalyst surface during reaction, suggest an alternative mechanism of deactivation.

Using DRIFTS, Persson *et al.* [35] reported an increase in signal intensity from surface hydroxyls weakly H-bonded to the support (3200–3800 cm^{-1}) [65] after introducing 1.5% CH_4 in air to a PdO/Al_2O_3 catalyst at low temperature (200 °C; Figure 9). The peak at 3016 cm^{-1} in Figure 9a, assigned to gas phase CH_4, increases with time-on-stream because of catalyst deactivation. The hydroxyls have characteristic adsorptions at 3733, 3697, 3556 and 3500 cm^{-1}, with the hydroxyls at 3697 and 3733 cm^{-1}

assigned to bridged and terminal isolated hydroxyl species, respectively. Upon CH_4 removal from the feed (Figure 9b), the peaks associated with OH species remain, highly consistent with a slow desorption of OH species produced during CH_4 oxidation. Hence, Persson *et al.* [35] suggested that catalyst deactivation on PdO/Al_2O_3 might be due to the formation and accumulation of hydroxyls on the catalyst surface, bound either to the PdO, Al_2O_3 or the interface between the two [30]. Gao *et al.* [32] reported similar hydroxyl bands at 3733, 3697, 3556 and 3500 cm^{-1} during lean-burn CH_4 oxidation (0.4% CH_4 in air) at 250 °C. The FTIR spectra from reaction with 2 vol.% H_2O added to the CH_4-O_2 feed also yield a broad band at 3445 cm^{-1} that is associated with OH species on Al_2O_3 [32].

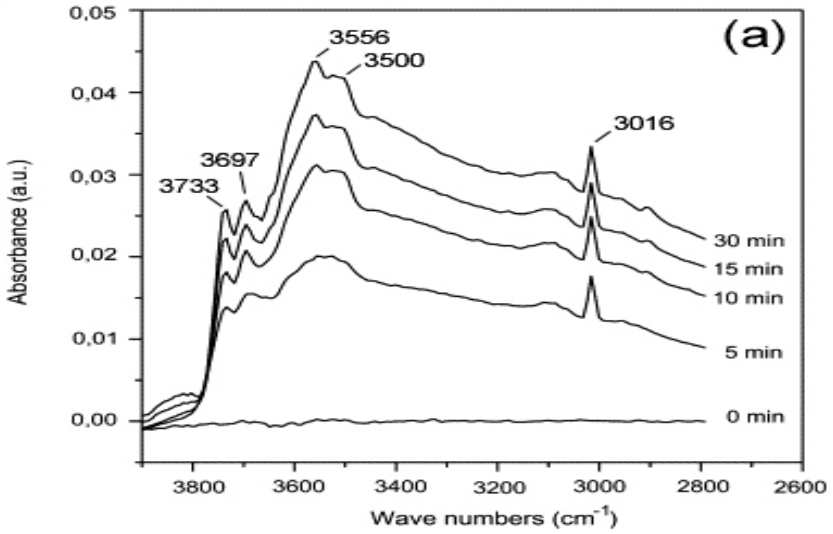

Figure 9. *Cont.*

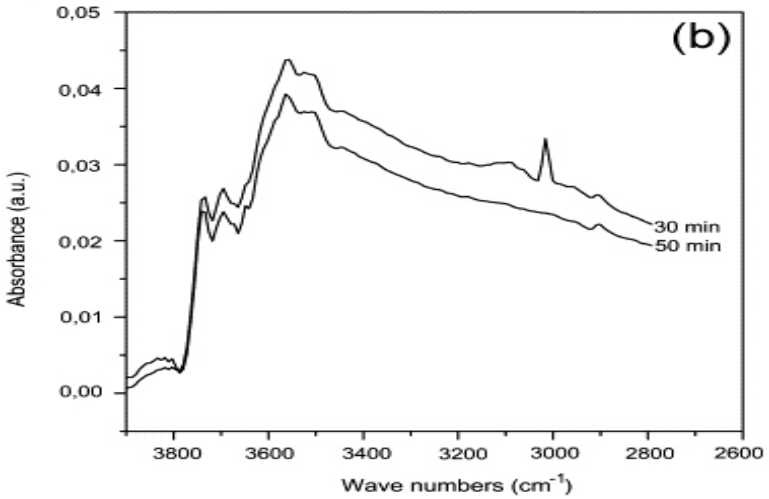

Figure 9. FTIR spectra of 5 wt.% Pd/Al_2O_3 at 200 °C (**a**) during the CH_4-O_2 reaction; (**b**) desorption when CH_4 was removed. Reproduced with permission from [35]. Copyright© 2007 Elsevier.

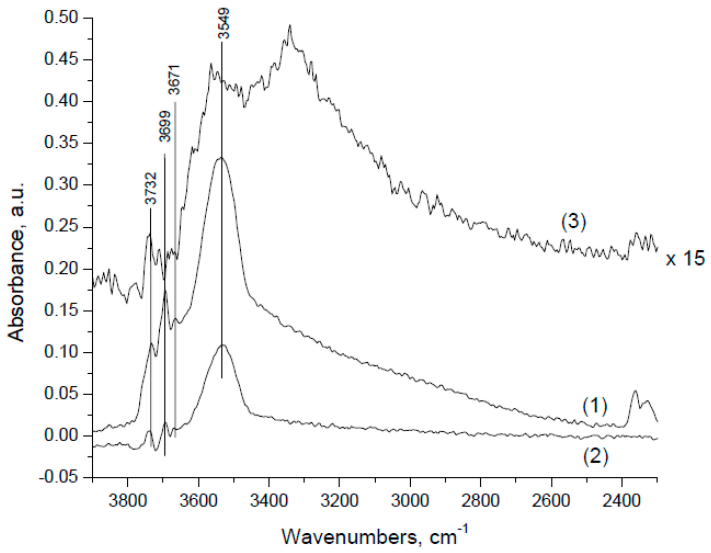

Figure 10. FTIR spectra at highest surface coverage and 350 °C on (1) PdO/Al_2O_3 during CH_4-O_2 reaction, (2) PdO/Al_2O_3 and (3) Al_2O_3 when injecting H_2O pulses. Reproduced with permission from [30]. Copyright © 2004 Elsevier.

Ciuparu *et al.* [30] also identified three well-defined peaks at 3732 (OH_I), 3699 (OH_{II}), and 3549 (OH_{III}) cm^{-1} associated with surface hydroxyls generated during CH_4 oxidation on a PdO/Al_2O_3 catalyst (3.5 wt % Pd) at 350 °C using a feed gas of 0.128% CH_4 and 17.3% O_2 in He/N_2 (Figure 10). The spectrum was compared to that measured at the same temperature when injecting pulses of ~3% H_2O into an air flow over the PdO/Al_2O_3 catalyst and the Al_2O_3 support (see Figure 10). Since Al_2O_3 has been shown to have a significantly lower hydroxyl coverage compared to PdO/Al_2O_3 when injecting H_2O pulses at 350 °C (the spectrum of Al_2O_3 is magnified by a factor of 15 in Figure 10), they concluded that the three peaks are associated with the presence of OH adsorbed on the PdO catalyst surface. The higher hydroxyl coverage during CH_4 oxidation compared to pulse injection of H_2O onto the PdO/Al_2O_3 catalyst, indicates that (1) adsorbed H_2O is dissociated on the surface of PdO/Al_2O_3 and (2) hydroxyls formed from H_2O pulses are less strongly bound to the surface than hydroxyls produced by the CH_4 oxidation reaction.

Since the frequencies of the OH_I and OH_{II} species are shifted to higher wave numbers for OH species more weakly bound to Pd, Ciuparu *et al.* [30] suggested that the high frequency peaks (OH_I, OH_{II}) can be assigned to terminal and bridged hydroxyl species, respectively, and the low frequency peak at ~3549 cm^{-1} with broad maximum values can be associated with OH species bound to different sites (multi-bound OHs; OH_{III}) (Figure 10). Transient temperature experiments show that the hydroxyl binding energy increases in the order $OH_I < OH_{II} < OH_{III}$ [30].

The peak areas of the terminal, bridged, and multi-bound hydroxyls were monitored with time-on-stream at different temperatures during reaction, as illustrated by Figure 11 for reaction at 175 °C [30]. Upon removal of CH_4 from the feed, the peak areas for the bridged and multi-bound OH species continue to increase, whereas the area of the terminal OH species decreases (Figure 11). This decrease is attributed to the conversion of terminal OH species to bridged or multi-bound OH species. Based on the intensities of the various hydroxyl species at different temperatures, the authors proposed the inter-conversion among the OH species as: $OH_{III} \leftrightarrow OH_{II} \leftrightarrow OH_I \rightarrow H_2O_{(g)}$ where only terminal

OH species recombine and desorb as H_2O and the transformation of bridged OH species to terminal OH species is the rate determining step (RDS) for hydroxyl desorption and hence low temperature CH_4 oxidation [30]. Importantly the authors show that the surface coverage by the hydroxyls (Figure 11) correlates with the activity loss at low temperature, meaning that the activity loss and surface coverage have similar timescales, from which they conclude that the former is likely an effect of the latter [30].

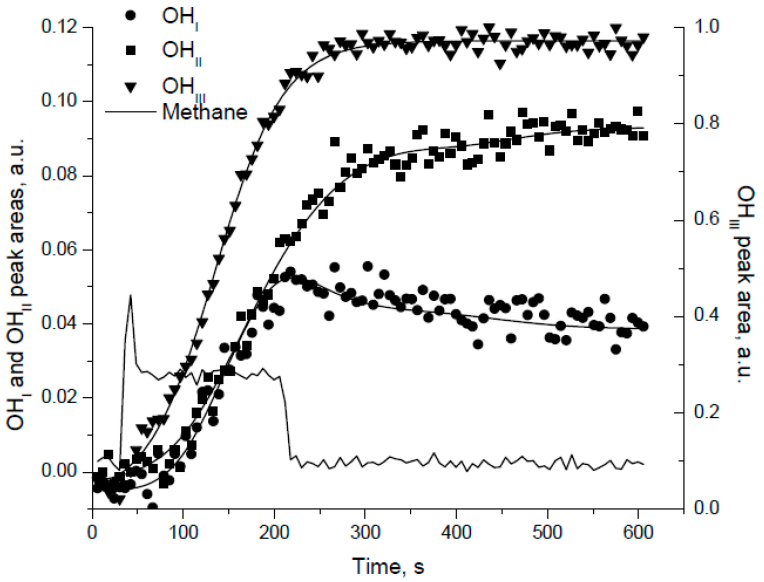

Figure 11. The normalized peak areas of different surface OH species generated during lean-CH_4-O_2 reaction at 175 °C. Reproduced with permission from [30]. Copyright © 2004 Elsevier.

FTIR spectra measured during CH_4 oxidation at 325 °C with 0.1% CH_4/4%O_2 in He over a series of 3 wt.% PdO catalysts supported on Al_2O_3, MgO, TiO_2 and MCM-41 [44] show that the hydroxyl coverage is dependent on the support. On Al_2O_3, well defined peaks similar to those identified by Ciuparu *et al.* [30] are observed, but no common peak among all catalysts that would provide evidence for Pd-OH bond formation, are present. Furthermore the large contribution from OH bonding on the supports makes it impossible to directly identify the presence of $Pd(OH)_2$ on these supports [32,44]. However, by using ^{18}O isotopic labeling and FTIR, the authors demonstrate that peaks associated with the accumulation of hydroxyls on PdO are not present at 325 °C. Hence, the more recent evidence suggests that deactivation by $Pd(OH)_2$ formation is unlikely, in agreement with the experimental observation that $Pd(OH)_2$/C decomposes in N_2 at about 250 °C [66]. In addition, evidence from temperature-programmed desorption studies of H_2O adsorbed on PdO(101) thin films, suggests the formation of an OH-H_2O complex at low temperature (<127 °C) and low coverage (< ½ monolayer), whereas H_2O preferentially chemisorbs in molecular form at higher coverages [67].

Schwartz *et al.* [44] showed, however, that catalyst deactivation during CH_4 oxidation correlates with hydroxyl accumulation on the oxide support. The redox mechanism for CH_4 combustion on Pd/PdO generally assumes dissociation of a CH_4 molecule to yield a methyl fragment and a hydroxyl group (CH_4 + Pd-O + Pd-*→Pd-OH + Pd-CH_3, where Pd-* represents a vacancy) [68,69]. H atoms are abstracted sequentially from the methyl group by neighboring Pd-O to form surface hydroxyl groups (Pd-OH). Recombination of surface hydroxyls yields water and a surface vacancy (2Pd-OH→H_2O +

Pd-O +Pd-*), that is regenerated by oxygen (2Pd-* + O_2→2Pd-O) [68,69]. Based on their experimental studies, Schwartz *et al.* [44,57], proposed that during lean-burn CH_4 oxidation, O_2 molecules dissociate on Pd-* sites and exchange with oxygen on the support so that Pd active sites are re-oxidized with oxygen atoms from the support during the catalytic reaction as follows:

$$\text{Pd-O} + \text{S-*} \leftrightarrow \text{Pd-*} + \text{S-O} \quad (1)$$

$$\text{Pd-*} + \text{S-O}^s \leftrightarrow \text{Pd-O}^s + \text{S-*} \quad (2)$$

and overall:

$$\text{Pd-O} + \text{S-O}^s \leftrightarrow \text{Pd-O}^s + \text{S-O} \quad (3)$$

where S represents the support, S-* is an O vacancy on the support and O^s represents an O atom associated with the solid oxide. This proposed mechanism suggests the possibility that a primary cause for catalyst deactivation is hydroxyl accumulation on the support, which hinders oxygen migration and exchange processes.

Evidence for O exchange with the support is provided by the isotopic labeling experiments summarized in Figure 12, during which $Pd^{18}O/Al_2{}^{16}O_3$ and $Pd^{18}O/Mg^{16}O$ were exposed to $^{18}O_2$/He flow at 400 °C [57]. An increase in $^{16}O^{18}O$ signal intensity with time is proposed to arise from oxygen exchange with the catalyst support [44]. The $^{16}O^{18}O$ signal (see lower, separate dashed line in Figure 12) is reduced when $H_2{}^{16}O$ is injected to the feed and is recovered when $H_2{}^{16}O$ is removed. Apparently, hydroxyl groups tend to migrate to the oxide support rather than desorb. By increasing the concentration of hydroxyl groups, through addition and dissociation of H_2O, oxygen exchange of Pd-* active sites with the oxide support (S-O^s) is interrupted. Thus, the number of PdO sites participating in the CH_4 oxidation reaction decreases with time, as H_2O dissociates and OH coverage of the support increases, with a consequent decrease in CH_4 conversion [44]. This proposed mechanism of catalyst deactivation is believed to occur at temperatures below 450 °C. Finally, the authors note that the rate of deactivation on Pd/Al_2O_3 catalysts, with higher concentrations of hydroxyl during reaction, is higher than on catalysts containing a support with higher oxygen mobility (Pd/MgO) [44,57].

Ciuparu *et al.* [70] also reported on pulsed experiments with $^{18}O_2$ over pure Pd and Pd/ZrO_2 catalysts, oxidized before reaction, to clarify the effect of hydroxyls on the surface oxygen exchange. They determined that due to the slow recombination of hydroxyls and hence H_2O desorption from the Pd catalyst surface during CH_4 oxidation (2Pd-OH→H_2O + Pd-O +Pd-*), the isotopic exchange of oxygen with the Pd sites (see Figure 13) occurs before H_2O desorption from the surface. The oxygen vacancies on the PdO surface resulting from H_2O desorption are thus rapidly filled by oxygen from the PdO bulk or oxide support (Pd-* + S-O^s↔Pd-O^s + S-*). In fact, in this unsteady-state experiment, the labeled oxygen pulsed through the catalyst bed, is purged from the reactor before H_2O is desorbed [70]. These observations are in agreement with the studies of Schwartz *et al.* [44,57] already discussed and confirm that the accumulation of hydroxyls on the Pd catalyst surface impedes the oxygen exchange and limits Pd catalyst activity.

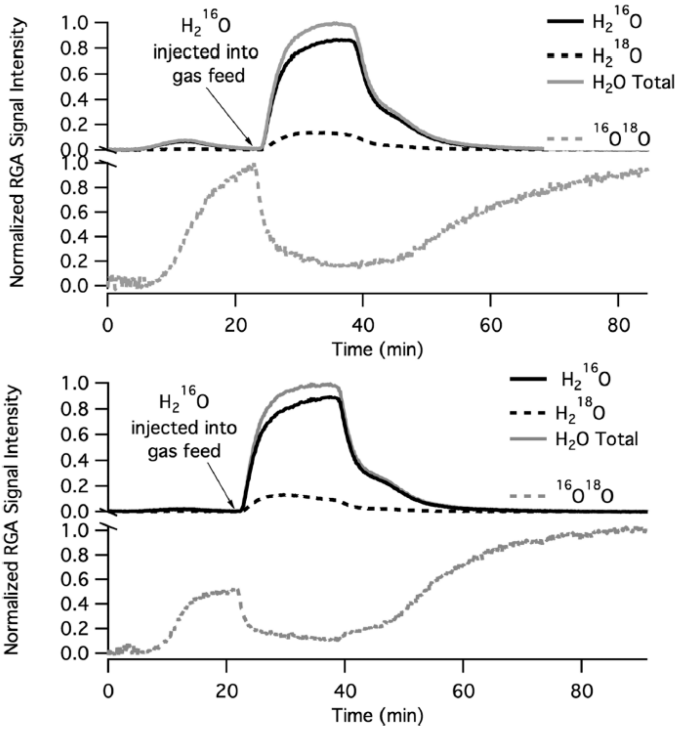

Figure 12. Oxygen exchange of (a) 3 wt.% $Pd^{18}O/Al_2{}^{16}O_3$ (top) and (b) 3 wt.% $Pd^{18}O/Mg^{16}O$ (bottom) with catalyst supports in a flow of $^{18}O_2$/He at 400 °C. $H_2{}^{16}O$ was injected at some time to probe its effect on oxygen exchange. Reproduced with permission from [44]. Copyright ©2012 American Chemical Society.

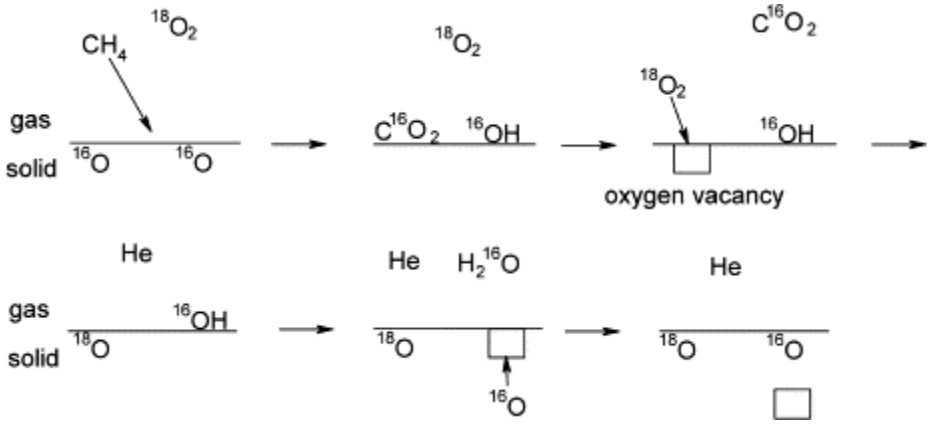

Figure 13. Schematic of oxygen exchange during CH_4 oxidation using labeled pulsed experiments. Reproduced with permission from [70]. Copyright © 2002 Elsevier.

3. The Use of Pd-Bimetallic Catalysts for CH_4 Oxidation

Pd-bimetallic catalysts have been studied to improve stability of Pd catalysts for CH_4 oxidation [19,51,71,72]. Pd-bimetallic catalysts are usually less active than Pd alone [64,73–75] simply because they contain less Pd, the most active metal for CH_4 oxidation [20,25]. The lower activity of the bimetallic compared to Pd alone may also be due to the presence of smaller amounts of PdO as a result of alloy formation between Pd and Pt [64], or the transformation of PdO to Pd metal [76]. According

to Ozawa *et al.* [77] the addition of Pt improves PdO/Al_2O_3 catalyst stability by preventing the growth of PdO and Pd–Pt particles during CH_4 oxidation at high temperature (800 °C) [77].

Several studies have reported higher initial activity of Pd-bimetallic catalysts compared to Pd alone [17,19,51,78]. These researchers suggest that the second metal added to Pd dissociates O_2 and the resulting O atoms are adsorbed by Pd, helping to maintain PdO active sites. Ishihara *et al.* [78] reported a T_{50} of 533 °C for a 1 wt.% Pd/Al_2O_3 catalyst, whereas for a Pd-Ni/Al_2O_3 catalyst (Pd:Ni = 9:1) T_{50} was 380 °C. In another study, it was reported that a higher dispersion of PdO on PdO-Pt/α-Al_2O_3 catalyst (27%) compared to PdO/α-Al_2O_3 (14%) results in higher initial activity and higher stability of the bimetallic catalyst [51] . After exposing the PdO/α-Al_2O_3 catalyst to the reaction feed stream for 6 h at 350 °C, an increase in average particle size from 8 to 11 nm is observed, whereas the average particle size does not change significantly for the PdO-Pt/α-Al_2O_3 catalyst [51].

Persson *et al.* [73] examined a series of Pd-bimetallics supported on Al_2O_3 finding that the metallic phase structure has a significant influence on the catalyst stability. For example, in several bimetallic systems (PdAg, PdCu, PdRh, and PdIr) separate phases of each metal oxide are formed after calcination (at 1000 °C for 1h followed by 1000 °C for 2h after loading the supported metal oxide powders onto a cordierite monolith) and this enhances catalyst stability in the case of the PdCu and PdAg (as measured stepwise at temperatures from 400–800 °C in 1.4% CH_4 in dry air at a space velocity of 250,000 h^{-1}). Formation of a Co or Ni aluminate spinel in PdCo and PdNi bimetallics, however, does not improve catalyst stability, whereas alloy formation in PdPt and PdAu on Al_2O_3 increases hydrothermal stability in the presence of 15% H_2O/air at 1000 °C for 10 h. In another study by Persson *et al.* [64], Pd-Pt bimetallic catalysts on various supports (alumina, zirconia) were shown to have higher thermal stability than monometallic Pd during CH_4 oxidation in dry air (1.5% CH_4 in air at a GHSV 250,000 h^{-1}). The stability of the Pd-Pt catalysts improved at lower temperatures (up to 620 °C). At temperatures of 520 °C and 570 °C CH_4 conversion on Pd-Pt catalysts increased with time-on-stream. Above 620 °C (especially at 670 °C and 720 °C) conversion decreased with time-on-stream. Those catalysts with higher initial activity also had higher deactivation rates. The deactivation cannot be attributed to PdO decomposition because the initial activity test showed that PdO decomposition started at higher temperature (770 °C with 1.5 vol.% CH_4 in air). According to XRD results, no PdO decomposition was observed at temperatures below 800 °C for the Pd/Al_2O_3, although PdO decomposition at ~700 °C may have yielded Pd that was not detectable by XRD (due to low concentration or high dispersion).

The amount of second metal added to the Pd can also affect the stability of the bimetallic catalyst. Persson *et al.* [74] reported that Pd-Pt bimetallic catalysts with Pd:Pt ratios of 2:1 and 1:1 are stable. Time-on-stream CH_4 oxidation experiments (in 1.5% CH_4 in air at a space velocity of 250,000 h^{-1}) for both a 5 wt.% Pd/Al_2O_3 and a 2:1 Pd:Pt/Al_2O_3 bimetallic with total metal loading of 5 wt.% were studied over a wide range of temperatures (470–720 °C) [64]. The temperature was increased from 470 °C to 720 °C stepwise by 50 °C and held for 1 h at each temperature. CH_4 conversion over the Pd/Al_2O_3 and Pd-Pt/Al_2O_3 catalyst decreased during the 1 h reaction time at each temperature. However, the decrease in conversion was lower for the bimetallic catalyst compared to the Pd catalyst. The decrease in activity was higher at higher temperatures (670 °C and 720 °C), especially for the Pd catalyst. *In situ* XRD spectra of the Pd-Pt bimetallic catalysts are shown in Figure 14. At room temperature, a sharp peak corresponding to Pd-Pt (111) and a small peak corresponding to PdO (101) are observed for

the PdPt-Al_2O_3 catalyst. By increasing the temperature to 300 °C, the PdO peak disappears and then reappears at 500 °C. The Pd-Pt peak intensity reaches a maximum at 700 °C while the PdO peak disappears at this temperature. The formation of Pd-Pt instead of PdO is consistent with deactivation of the bimetallic catalyst at high temperature (700 °C).

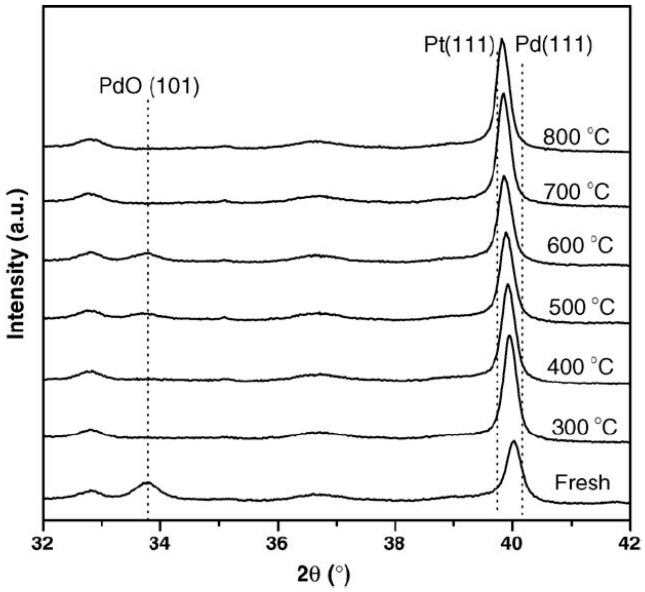

Figure 14. High-temperature *in situ* XRD profiles of PdPt-Al_2O_3 during heating. Reprinted with permission from [64]. Copyright © 2006 Elsevier.

Steady-state experiments using a 18.7 wt.% Pd/Al_2O_3 catalyst with different loadings of Pt (1.6, 3.1 and 3.9 wt.%) (Figure 15) reported by Ozawa *et al.* [77], also provide some insight into the improved stability of bimetallic catalysts as Pt content increases. In this study, reaction temperature was held at 800 °C and CH_4 combustion rate was measured over a 10 h period using a 1% CH_4 in air feed gas at a GHSV of 1,500,000 mL/(g_{cat}-h). Deactivation rate is shown to decrease as the Pt loading of the Pd-Pt bimetallics increases. For example, the combustion rate for the 18 wt.% Pd-3.9 wt.% Pt/Al_2O_3 decreases from 710 μmol s^{-1} g^{-1} to 460 μmol s^{-1} g^{-1} after 10 h, whereas it decreases to 400 μmol s^{-1} g^{-1} for the 18.4 wt.% Pd-1.6 wt.% Pt/Al_2O_3 catalyst.

XRD analysis of the catalysts studied by Ozawa *et al.* [77] after 10 h reaction indicates PdO to be present in the Pt-doped catalysts while no Pd^0 is observed. However, Pd^0 is present in the Pd monometallic catalyst, likely because of the decomposition of PdO at the high temperature of the reaction (800 °C). In addition, the crystallite size of the PdO (101) in the Pd catalyst is larger than for the Pd-Pt catalysts. Table 4 compares changes in PdO particle size and BET surface area before and after 10 h reaction for the same Pd and Pd-Pt catalysts. From these data it is clear that the extent of sintering of the Pd catalyst is greater than for the Pd-Pt catalysts. The time-on-stream conversion data reported by Ozawa *et al.* [77] (Figure 15) were fitted to a deactivation equation with two terms, the first representing rapid transformation of PdO to Pd^0 of the Pd-Pt alloy phase, and the second associated with the slow growth of the PdO crystallite [77]. The deactivation is affected more by the second term suggesting that particle growth of the PdO is the main cause of catalyst deactivation at the chosen reaction conditions [77].

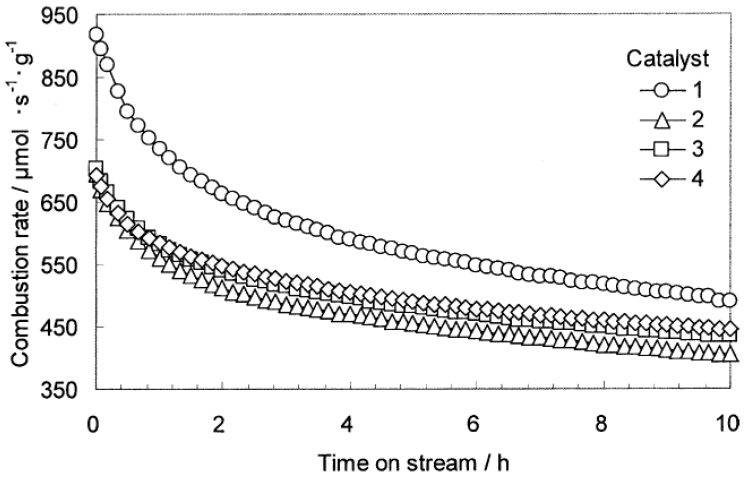

Figure 15. CH_4 combustion rate at 800 °C with time on stream. Combustion conditions: 1 vol.% CH_4, 99 vol.% air, CH_4/air flow = 450 L.h^{-1}, catalyst weight = 0.3 g. Catalyst 1, 2, 3, and 4 represent 18.7 wt.% Pd, 18.4 wt.% Pd-1.6 wt.% Pt, 18.1 wt.% Pd-3.4 wt.% Pt, and 18.0 wt.% Pd-3.9 wt.% Pt over Al_2O_3 catalysts. Reprinted with permission from [77]. Copyright © 2004 Elsevier.

Table 4. Changes in Pd and Pt-Pd catalyst properties before and after aging. Adapted from [77].

Catalyst, wt.% on Al_2O_3		**18.7% Pd**	**18.4% Pd-1.6% Pt**	**18.1% Pd-3.1% Pt**	**18.0% Pd-3.9% Pt**
BET area, m^2/g	Fresh	56	51	51	46
	Aged	46	46	46	52
PdO size, nm	Fresh	12.5	15.3	15.2	14.7
	Aged	17.9	18.0	16.7	16.2

These results are in a good agreement with the results reported by Yamamoto *et al.* [72] in which a Pd-Pt bimetallic catalyst was more active for CH_4 conversion than Pd (as measured by the temperature required for 50% CH_4 conversion) and the conversion was maintained following 2500 h time-on-stream at 385 °C. XRD analyses showed that the crystallite growth as a function of time for both Pd (111) and PdO (101) was faster on the Pd (10 g/L)/Al_2O_3 catalyst than the Pd(10 g/L)-Pt (10 g/L)/Al_2O_3 catalyst. Hence one concludes that the presence of Pt retards the sintering of PdO.

Effects of H_2O on deactivation of Pt *versus* Pt-Pd catalysts have also been reported, at both thermal and hydrothermal aging conditions [17,19,71]. Pieck *et al.* [17] reported that the T_{50} of a 0.4% Pt-0.8% Pd/Al_2O_3 catalyst after thermal treatment at 600 °C for 4 h in wet air (60 cm^3 min^{-1} air flow with 0.356 cm^3 h^{-1} water), is ~50 °C lower than that obtained over a Pd catalyst. Lapisardi *et al.* [19] reported that a fresh $Pd_{0.93}$-$Pt_{0.07}$/Al_2O_3 catalyst (total metal loading 2.12 wt.% with Pd:Pt molar ratio of 0.93:0.07) is as active as a fresh Pd/Al_2O_3 catalyst in a dry feed [19]. Interestingly, the $Pd_{0.93}$-$Pt_{0.07}$/Al_2O_3 catalyst is less affected by addition of 10 vol.% steam to the feed stream than the 2.2 wt.% Pd/Al_2O_3 catalyst. The T_{50} for the Pd-Pt bimetallic increases from 320 °C to 400 °C when 10 vol.% steam is added to the feed stream, whereas the corresponding increase in T_{50} for the Pd/Al_2O_3

catalyst is from 320 °C to 425 °C. Thus, the Pd-Pt bimetallic, containing only 0.26 wt % Pt is more active and stable than the Pd catalyst for CH_4 oxidation in the presence of steam.

The stabilities of Pt and Pt-Pd catalysts each loaded on a wash coated monolith have also been reported [71]. A feed stream with 4067 ppmv CH_4 in air was reacted over these catalysts as reaction temperature increased from 300 to 700 °C stepwise in 50 °C increments. CH_4 conversion was monitored for a period of 1 h at each temperature. Subsequently the temperature was decreased to 300 °C also in 50 °C steps, again holding at each temperature for 1 h. The conversion of CH_4 was compared for both heating and cooling cycles. The results show that the Pt-Pd catalyst is more active than the Pt catalyst. The comparison between the heating and cooling cycles was also done for steam-aged catalysts, in which the catalysts were exposed to the feed stream at 650 °C with 5 vol.% water for 20 h. Table 5 lists the T_{50} for both fresh Pt and Pd-Pt catalysts, the steam-aged catalysts during tests in a dry feed and the steam-aged catalysts tested in a wet feed, containing 5 wt % H_2O. The data show that the fresh Pd-Pt catalyst is more active than the fresh Pt catalyst. Higher activities are also observed for steam-aged Pd-Pt catalysts tested in dry or wet feed gas.

Table 5. T_{50} for fresh and steam aged Pd and Pt-Pd catalysts operated in dry and wet feed. Combustion conditions: 4067 vol. ppm CH_4; total flow rate of 234.5 cm^3/min; 500 mg catalyst; 5 vol.% water in wet feed. Adapted from [71].

Catalyst	Temperature at 50% CH_4 conversion (T_{50}), °C		
	Fresh	Steam-aged	Steam-aged
	Dry feed	Dry feed	Wet feed
Pt	540	610	610
4:1 Pt-Pd	400	470	535

4. Kinetic Consequences of H_2O on CH_4 Oxidation over Pd Catalysts

The rate of CH_4 oxidation over Pd catalysts is influenced by temperature, reactant partial pressures, the state of the Pd at reaction conditions (Pd^0, PdO or a sub-oxide), possibly Pd crystallite size (*i.e.*, may be structure-sensitive), and inhibition by products H_2O and CO_2. Consequently, kinetic parameters reported in the literature vary over wide ranges; this is especially true of the apparent activation energy for CH_4 oxidation [20]. As noted by Carstens *et al.* [79], rate data must account for the inhibition effect of H_2O when determining the activation barrier, but Ciuparu *et al.* [43] has shown that the correction is complicated by the fact that the effect of H_2O inhibition is temperature dependent. For example, the apparent activation energy for CH_4 oxidation over a Pd/ZrO_2 catalyst is estimated to be 180 kJ/mol from data measured at temperatures below 192 °C, whereas a value of 87 kJ/mol is obtained at temperatures above 192 °C [42]. The higher value of the apparent activation energy at lower temperatures is attributed to the strong inhibiting effect of H_2O on the Pd catalyst.

Zhu *et al.* [80] reported kinetic parameters for CH_4 oxidation over a series of model Pd and PdO surfaces and foils, and compared the values to literature data on supported Pd catalysts (Table 6). From Table 6 the reaction orders for CH_4 and O_2 are probably not sensitive to the structure of the Pd catalyst,

although on the supported catalysts the reaction orders for H_2O vary from −0.25 to −1.3. Taking account of the error in the E_a estimates (±20 kJ/mol), Zhu *et al.* [80] concluded that on the large single-crystal model catalysts, the activation energies are similar and the combustion of CH_4 over Pd or PdO is not sensitive to the structure of the catalyst. Larger E_a values are reported for the Pd/oxide-supports (150–185 kJ/mol) corrected for the effect of H_2O (assuming an order of −1) [79], whereas the much smaller E_a for the Pd/zeolite catalysts (72–77 kJ/mol) are possibly associated with the high acidity and high OH surface concentration of zeolites, in obvious contrast to the observed inhibition by OH groups for PdO supported on conventional supports. The negative orders of reaction for H_2O are indicative of the varying degrees of inhibition of CH_4 oxidation by H_2O on Pd and PdO surfaces and catalysts.

Table 6. Kinetic parameters for CH_4 oxidation over Pd catalysts.

Catalyst	E_a,	Reaction order			*T* Range	Refs
	kJ/mol	CH_4	O_2	H_2O	°C	
Model Catalysts						
Pd foil	125	0.7	−0.1	0.05	296–360	[81]
Pd (111)	140	0.7	−0.1	0.05	296–360	[80]
Pd (100)	130	0.9	0.01	0.07	296–360	[80]
PdO foil	125	0.7	0.2	−0.9	296–360	[80]
PdO(111)	140	0.8	−0.1	−0.9	296–360	[80]
PdO(100)	125	0.8	0.1	−1.0	296–360	[80]
Supported Catalysts						
Pd black	135	0.7	0.1	−0.8	296–360	[81]
8.5% Pd/Al_2O_3	150	1	0	-1	232–360	[80,82]
0.5% Pd/Al_2O_3[a]	60	0.90	0.08	−1.3 to −0.9	240–400	[83]
10% Pd/ZrO_2	185	1	0	−1	232–360	[80,82]
5% Pd/ZrO_2	185	1.1	0.1	−1.0	250–280	[68]
1% Pd/ZrO_2	172	1	0	−1.0	227–441	[53]
1% Pd/SiO_2	-	1	0	−0.25	227–441	[53]
2.8% Pd/H-Mord.	77	0.7	-0.1	−0.4	342–417	[33]
2.5% Pd-H-beta	72	0.5	0.2	−0.5	342–417	[33]

[a] E_a determined under dry reaction conditions, correction for H_2O inhibition.

The role of H_2O in the inhibition of PdO catalysts during CH_4 oxidation has been documented in this review to relate to the adsorption and slow desorption of H_2O on active sites during reaction. Kikuchi *et al.* [16] proposed a kinetic model assuming competitive adsorption between H_2O and CH_4 on PdO sites, where dissociative CH_4 adsorption was assumed to be the rate determining step (RDS) and the coverage by C-species was assumed to be negligible. The main elementary steps of the reaction are postulated as follows:

$$H_2O_{(g)} + s \rightarrow H_2O - s \quad (4)$$

$$CH_{4(g)} + 2s \rightarrow CH_3 - s + H - s \quad (5)$$

from which the following rate expression is derived [16]:

$$r = k_r \frac{P_{CH_4}}{1 + K_{H_2O} P_{H_2O}} \quad (6)$$

where r is the reaction rate, k_r is the rate constant for H abstraction, K_{H_2O} is the H_2O adsorption equilibrium constant, and P_{CH_4} and P_{H_2O} are the partial pressures of CH_4 and H_2O, respectively. K_{H_2O} is exponentially dependent upon the H_2O adsorption enthalpy (ΔH_{ads}). To increase the activity and durability of the Pd catalysts in the presence of H_2O, K_{H_2O} should be small according to the above reaction model. Based on the measured ΔH_{ads} values for water on supported Pd catalysts, water adsorbed on Pd/Al_2O_3 has the highest negative adsorption enthalpy ($\Delta H_{ads} = -49$ kJ mol^{-1}) compared to Pd/SnO_2 (-31 kJ mol^{-1}) and Pd/Al_2O_3-36NiO (-30 kJ mol^{-1}) (Table 7) despite the lower activation energy calculated for Pd/Al_2O_3 (see Table 7) [16]. A higher $|\Delta H_{ads}|$ implies stronger H_2O adsorption on the surface and is evidence of a higher coverage of active sites by H_2O molecules on Pd/Al_2O_3 catalysts and consequently lower catalyst activity. However, the larger negative enthalpy also predicts a more rapid decrease in K_{H2O} with increasing temperature for Pd/Al_2O_3.

Table 7. Estimated kinetic parameters for CH_4 oxidation using the rate equation $r = k_r \frac{P_{CH_4}}{1+K_{H_2O}P_{H_2O}}$ [16].

Catalyst	Pd loading (wt.%)	E_a kJ/mol	ΔH_{ads} for H_2O kJ/mol
Pd/Al_2O_3	1.1	81	−49
Pd/SnO_2	1.1	111	−31
Pd/Al_2O_3-36NiO	1.1	90	−30

The larger negative value in the order of H_2O for the 1% Pd/ZrO_2 catalyst, compared to the Pd/SiO_2 catalyst, as reported by Araya *et al.* [53] (Table 6), reflects stronger H_2O adsorption on ZrO_2 than on the SiO_2 [53]. Hurtado *et al.* [83] observed a change in the power-law reaction order of H_2O from −1.3 to −0.9 as temperature increased from 300 °C to 350 °C using a H_2O-CH_4-O_2 reactant mixture and a commercial 0.5 wt.% Pd/γ-Al_2O_3 catalyst. Considering the equation proposed by Kikuchi *et al.* [16],

with $K_{H_2O}P_{H_2O} \gg 1$, the H_2O reaction order will reduce to −1 but if $K_{H_2O}P_{H_2O}$ is small, the H_2O reaction order reduces to a value approaching zero.

Hurtado *et al.* [83] also attributed the inhibition effect of H_2O during reaction to the adsorption of H_2O on Pd catalysts. Based on this assumption the authors examined several Eley-Rideal, Langmuir-Hinshelwood and Mars-van Krevelen kinetic models finding that by considering competitive adsorption between H_2O and CH_4 on Pd oxide sites and slow desorption of products, the following kinetic model could be derived:

$$r = \frac{k_1 k_2 P_{CH_4} P_{O_2}}{k_1 P_{O_2}(1+K_{H_2O}P_{H_2O})+2k_2 P_{CH_4}+(k_1 k_2/k_3)P_{O_2}P_{CH_4}} \quad (7)$$

where k_1, k_2, and k_3 are the rate constants for (1) irreversible oxygen adsorption, (2) surface reaction with CH_4, and (3) product desorption steps in the mechanistic sequence, respectively. This model provides the best fit of their measured rate data. The ΔH_{ads} for water estimated from equation (7) is −54.5 kJ/mol, in agreement with the data of Table 7. The inhibiting effects of H_2O are assumed to be a consequence of a competitive adsorption between CH_4 and H_2O on PdO sites. Deactivation by H_2O was previously thought to be due to formation of inactive $Pd(OH)_2$ that does not participate in the CH_4 oxidation reaction and is reversible at temperatures above 250 °C [66]. Hurtado *et al.* [83] also note that the formation of $Pd(OH)_2$ is thermodynamically favored from PdO sites rather than from Pd^0. However, the more recent mechanism involving H_2O inhibition of the O exchange between Pd sites and oxide supports, proposed by Schwartz *et al.* [44,57] (see earlier discussion) appears to be supported by more definitive data.

5. Conclusions

Studies of the past decade provide new insights into the effects of H_2O on Pd catalysts during CH_4 oxidation, especially at lower temperatures. The principal effects of H_2O are:

(a) reaction inhibition by H_2O adsorption
(b) deactivation due to formation of $Pd(OH)_2$ and
(c) H_2O-assisted sintering at high reaction temperatures (>500 °C)

Reaction inhibition by H_2O increases with (a) decreasing reaction temperature at <500 °C and (b) higher H_2O concentrations, while this effect is generally negligible at >500 °C. O surface mobility of supports apparently influences H_2O inhibition, *i.e.*, high O mobility (on CeO_2 and ZrO_2) results in less inhibition by H_2O than for Al_2O_3.

The main cause of partially reversible deactivation has been related to hydroxyl adsorption on the support and PdO. Although earlier studies suggested that formation of inactive $Pd(OH)_2$ could be the cause of deactivation, recent studies provide definitive evidence that adsorbed hydroxyls suppress O exchange between the support and Pd active sites causing suppression of catalyst activity.

H_2O-assisted sintering of supported Pd catalysts is observed at >500 °C. Catalysts with stabilized supports or core-shell structures have higher resistance to hydrothermal sintering. Several studies show that Pd bimetallic catalysts also improve catalyst stability, although explanations for the role of the second metal are not well-defined. Suppression of PdO sintering, enhanced oxygen mobility and suppression of hydroxide formation are postulated to play a key role in higher stability of Pd bimetallic catalysts.

Rate expressions from kinetic studies of CH_4 oxidation at conditions relevant to natural gas vehicles are based on the assumptions of (a) product inhibition by H_2O is a consequence of a competitive adsorption mechanism between CH_4 and H_2O on PdO sites; and (b) deactivation by H_2O is due to the formation of inactive $Pd(OH)_2$. None of the previous kinetic studies have linked the observed kinetic effects of H_2O to O mobility that recent studies show is critical during CH_4 oxidation.

Acknowledgements

The financial support of Westport Innovations Inc. and Natural Sciences and Engineering Research Council of Canada (NSERC) is gratefully acknowledged.

References

1. US Government. The World Factbook 2013–14. Washington, DC: Central Intelligence Agency, 2013. Available online: https://www.cia.gov/library/publications/the-world-factbook/geos/xx.html (accessed on 1 September 2013).
2. Natural Gas Vehicle Knowledge Base, Statistics. Available online: http://www.iangv.org/category/stats/ 2014 (Accessed on 25 March 2015).
3. Bartholomew, C.H.; Farrauto, R.J. *Fundamentals of Industrial Catalytic Processes*, 2nd ed.; J. Wiley and Sons Inc: Hoboken, NJ, USA, 2006.
4. Barbier, J., Jr.; Duprez, D. Steam Effects in Three-Way Catalysis. *Appl. Catal. B* **1994**, *4*, 105–140.
5. Lox, E.S.J.; Engler, B.H. In *Handbook of Heterogeneous Catalysis*; Ertl, G., Knozinger, H., Weitkamp, J., Eds.; Wiley-VCH: Weinheim, Germany, 1997; Volume 4.
6. Ciuparu, D.; Lyubovsky, M.R.; Altman, E.; Pfefferle, L.D.; Datye, A. Catalytic Combustion of Methane over Palladium-Based Catalysts. *Catal. Rev. Sci. Eng.* **2002**, *44*, doi:10.1081/CR-120015482.
7. Silver, R.G.; Summers, J.C. In *Catalysis and Automotive Pollution Control III Studies in Surface Science and Catalysis*; Frennet, A., Bastin, J.M., Eds.; Elsevier Science: Amsterdam, The Netherlands, 1995; pp. 871–884.
8. Klingstedt, F.; Neyestanaki, A.K.; Byggningsbacka, R.; Lindfors, L.; Lundén, M.; Petersson, M.; Tengström, P.; Ollonqvist, T.; Väyrynen, J. Palladium Based Catalysts for Exhaust Aftertreatment of Natural Gas Powered Vehicles and Biofuel Combustion. *Appl. Catal. A* **2001**, *209*, 301–316.
9. Farrauto, R.J.; Hobson, M.C.; Kennelly, T.; Waterman, E.M. Catalytic Chemistry of Supported Palladium for Combustion of Methane. *Appl. Catal. A* **1992**, *81*, 227–237.
10. Lampert, J.K.; Kazi, M.S.; Farrauto, R.J. Palladium Catalyst Performance for Methane Emissions Abatement from Lean Burn Natural Gas Vehicles. *Appl. Catal. B* **1997**, *14*, 211–223.
11. Bounechada, D.; Groppi, G.; Forzatti, P.; Kallinen, K.; Kinnunen, T. Effect of Periodic lean/rich Switch on Methane Conversion over a Ce–Zr Promoted Pd-Rh/Al_2O_3 catalyst in the Exhausts of Natural Gas Vehicles. *Appl. Catal. B* **2012**, *119–120*, 91–99.
12. Gelin, P.; Primet, M. Complete Oxidation of Methane at Low Temperature over Noble Metal Based Catalysts: A Review. *Appl. Catal. B* **2002**, *39*, 1–37.

13. Choudhary, T.V.; Banerjee, S.; Choudhary, V.R. Catalysts for Combustion of Methane and Lower Alkanes. *Appl. Catal. A* **2002**, *234*, 1–23.
14. Centi, G. Supported Palladium Catalysts in Environmental Catalytic Technologies for Gaseous Emissions. *J. Mol. Catal. A* **2001**, *173*, 287–312.
15. Forzatti, P.; Groppi, G. Catalytic Combustion for the Production of Energy. *Catal. Today* **1999**, *54*, 165–180.
16. Kikuchi, R.; Maeda, S.; Sasaki, K.; Wennerström, S.; Eguchi, K. Low-Temperature Methane Oxidation over Oxide-Supported Pd Catalysts: Inhibitory Effect of Water Vapor. *Appl. Catal. A* **2002**, *232*, 23–28.
17. Pieck, C.L.; Vera, C.R.; Peirotti, E.M.; Yori, J.C. Effect of Water Vapor on the Activity of Pt-Pd/Al_2O_3 Catalysts for Methane Combustion. *Appl. Catal. A* **2002**, *226*, 281–291.
18. Roth, D.; Gélin, P.; Primet, M.; Tena, E. Catalytic Behaviour of Cl-Free and Cl-Containing Pd/Al_2O_3 Catalysts in the Total Oxidation of Methane at Low Temperature. *Appl. Catal. A* **2000**, *203*, 37–45.
19. Lapisardi, G.; Urfels, L.; Gélin, P.; Primet, M.; Kaddouri, A.; Garbowski, E.; Toppi, S.; Tena, E. Superior Catalytic Behaviour of Pt-Doped Pd Catalysts in the Complete Oxidation of Methane at Low Temperature. *Catal. Today* **2006**, *117*, 564–568.
20. Li, Z.; Hoflund, G.B. A Review on Complete Oxidation of Methane at Low Tempertaure. *J. Nat. Gas Chem.* **2003**, *12*, 153–160.
21. Colussi, S.; Gayen, A.; Camellone, M.F.; Boaro, M.; Llorca, J.; Fabris, S.; Trovarelli, A. Nanofaceted Pd-O Sites in Pd-Ce Surface Superstructures: Enhanced Activity in Catalytic Combustion of Methane. *Angew. Chem. Int. Ed.* **2009**, *48*, 8633–8636.
22. Cargnello, M.; Jaén, J.J.D.; Garrido, J.C.H.; Bakhmutsky, K.; Montini, T.; Gámez, J.J.C.; Gorte, R.J.; Fornasiero, P. Exceptional Activity for Methane Combustion over Modular Pd@CeO_2 Subunits on Functionalized Al_2O_3. *Science* **2012**, *337*, 713–717.
23. Hellman, A.; Resta, A.; Martin, N.M.; Gustafson, J.; Trinchero, A.; Carlsson, P.-A.; Balmes, O.; Felici, R.; van Rijn, R.; Frenken, J.W.M.; Andersen, J.N.; Lundgren, E.; Gronbeck, H. The Active Phase of Palladium during Methane Oxidation. *J. Phys. Chem. Lett.* **2012**, *3*, 678–682.
24. Briot, P.; Primet, M. Catalytic Oxidation of Methane over Palladium Supported on Alumina: Effect of Aging Under Reactants. *Appl. Catal.* **1991**, *68*, 301–314.
25. Gélin, P.; Urfels, L.; Primet, M.; Tena, E. Complete Oxidation of Methane at Low Temperature over Pt and Pd Catalysts for the Abatement of Lean-Burn Natural Gas Fuelled Vehicles Emissions: Influence of Water and Sulphur Containing Compounds. *Catal. Today* **2003**, *83*, 45–57.
26. Bartholomew, C.H. Mechanisms of Catalyst Deactivation. *Appl. Catal. A* **2001**, *212*, 17–60.
27. Kang, S.; Han, S.; Nam, S.; Nam, I.; Cho, B.; Kim, C.; Oh, S. Effect of Aging Atmosphere on Thermal Sintering of Modern Commercial TWCs. *Top. Catal.* **2013**, *56*, 298–305.
28. Shinjoh, H. Noble Metal Sintering Suppression Technology in Three-Way Catalyst: Automotive Three-Way Catalysts with the Noble Metal Sintering Suppression Technology Based on the Support Anchoring Effect. *Catal. Surv. Asia* **2009**, *13*, 184–190.
29. Fathali, A.; Olsson, L.; Ekstrom, F.; Laurell, M.; Andersson, B. Hydrothermal Aging-Induced Changes in Washcoats of Commercial Three-Way Catalysts. *Top. Catal.* **2013**, *56*, 323–328.

30. Ciuparu, D.; Perkins, E.; Pfefferle, L. *In Situ* DR-FTIR Investigation of Surface Hydroxyls on γ-Al_2O_3 Supported PdO Catalysts during Methane Combustion. *Appl. Catal. A* **2004**, *263*, 145–153.
31. Burch, R.; Urbano, F.J.; Loader, P.K. Methane Combustion Over Palladium Catalysts: The Effect of Carbon Dioxide and Water on Activity. *Appl. Catal. A* **1995**, *123*, 173–184.
32. Gao, D.; Wang, S.; Zhang, C.; Yuan, Z.; Wang, S. Methane Combustion over Pd/Al_2O_3 Catalyst: Effects of Chlorine Ions and Water on Catalytic Activity. *Chin. J. Catal.* **2008**, *29*, 1221–1225.
33. Park, J.; Kim, B.; Shin, C.; Seo, G.; Kim, S.; Hong, S. Methane Combustion over Pd Catalysts Loaded on Medium and Large Pore Zeolites. *Top. Catal.* **2009**, *52*, 27–34.
34. Stasinska, B.; Machocki, A.; Antoniak, K.; Rotko, M.; Figueiredo, J.L.; Gonçalves, F. Importance of Palladium Dispersion in Pd/Al_2O_3 Catalysts for Complete Oxidation of Humid Low-methane–air Mixtures. *Catal. Today* **2008**, *137*, 329–334.
35. Persson, K.; Pfefferle, L.D.; Schwartz, W.; Ersson, A.; Järås, S.G. Stability of Palladium-Based Catalysts during Catalytic Combustion of Methane: The Influence of Water. *Appl. Catal. B* **2007**, *74*, 242–250.
36. Liu, Y.; Wang, S.; Gao, D.; Sun, T.; Zhang, C.; Wang, S. Influence of Metal Oxides on the Performance of Pd/Al_2O_3 Catalysts for Methane Combustion Under Lean-Fuel Conditions. *Fuel Process. Technol.* **2013**, *111*, 55–61.
37. Zhu, G.; Han, J.; Zemlyanov, D.Y.; Ribeiro, F.H. Temperature Dependence of the Kinetics for the Complete Oxidation of Methane on Palladium and Palladium Oxide. *J. Phys. Chem. B* **2005**, *109*, 2331–2337.
38. Okumura, K.; Shinohara, E.; Niwa, M. Pd Loaded on High Silica Beta Support Active for the Total Oxidation of Diluted Methane in the Presence of Water Vapor. *Catal. Today* **2006**, *117*, 577–583.
39. Nomura, K.; Noro, K.; Nakamura, Y.; Yoshida, H.; Satsuma, A.; Hattori, T. Combustion of a Trace Amount of CH_4 in the Presence of Water Vapor over ZrO_2-Supported Pd Catalysts. *Catal. Lett.* **1999**, *58*, 127–130.
40. Cullis, C.F.; Nevell, T.G.; Trimm, D.L. Role of the Catalyst Support in the Oxidation of Methane over Palladium. *Faraday Trans*. **1972**, *68*, 1406–1412.
41. Eriksson, S.; Boutonnet, M.; Järås, S. Catalytic Combustion of Methane in Steam and Carbon Dioxide-Diluted Reaction Mixtures. *Appl. Catal. A* **2006**, *312*, 95–101.
42. Ciuparu, D.; Katsikis, N.; Pfefferle, L. Temperature and Time Dependence of the Water Inhibition Effect on Supported Palladium Catalyst for Methane Combustion. *Appl. Catal. A* **2001**, *216*, 209–215.
43. Ciuparu, D.; Pfefferle, L. Support and Water Effects on Palladium Based Methane Combustion Catalysts. *Appl. Catal. A* **2001**, *209*, 415–428.
44. Schwartz, W.R.; Ciuparu, D.; Pfefferle, L.D. Combustion of Methane over Palladium-Based Catalysts: Catalytic Deactivation and Role of the Support. *J. Phys. Chem. C* **2012**, *116*, 8587–8593.
45. Hansen, T.W.; DeLaRiva, A.T.; Challa, S.R.; Datye, A.K. Sintering of Catalytic Nanoparticles: Particle Migration Or Ostwald Ripening? *Acc. Chem. Res.* **2013**, *46*, 1720–1730.

46. Lamber, R.; Jaeger, N.; Schulz-Ekloff, G. Metal-Support Interaction in the Pd/SiO_2 System: Influence of the Support Pretreatment. *J. Catal.* **1990**, *123*, 285–297.
47. Nagai, Y.; Hirabayashi, T.; Dohmae, K.; Takagi, N.; Minami, T.; Shinjoh, H.; Matsumoto, S. Sintering Inhibition Mechanism of Platinum Supported on Ceria-Based Oxide and Pt-oxide–support Interaction. *J. Catal.* **2006**, *242*, 103–109.
48. Xu, Q.; Kharas, K.C.; Croley, B.J.; Datye, A.K. The Sintering of Supported Pd Automotive Catalysts. *ChemCatChem* **2011**, *3*, 1004–1014.
49. Escandón, L.S.; Niño, D.; Díaz, E.; Ordóñez, S.; Díez, F.V. Effect of Hydrothermal Ageing on the Performance of Ce-Promoted PdO/ZrO_2 for Methane Combustion. *Catal. Commun.* **2008**, *9*, 2291–2296.
50. Muto, K.; Katada, N.; Niwa, M. Complete Oxidation of Methane on Supported Palladium Catalyst: Support Effect. *Appl. Catal. A* **1996**, *134*, 203–215.
51. Narui, K.; Yata, H.; Furuta, K.; Nishida, A.; Kohtoku, Y.; Matsuzaki, T. Effects of Addition of Pt to PdO/Al_2O_3 Catalyst on Catalytic Activity for Methane Combustion and TEM Observations of Supported Particles. *Appl. Catal. A* **1999**, *179*, 165–173.
52. Zhang, B.; Wang, X.; M'Ramadj, O.; Li, D.; Zhang, H.; Lu, G. Effect of Water on the Performance of Pd-ZSM-5 Catalysts for the Combustion of Methane. *J. Nat. Gas Chem.* **2008**, *17*, 87–92.
53. Araya, P.; Guerrero, S.; Robertson, J.; Gracia, F.J. Methane Combustion over Pd/SiO_2 Catalysts with Different Degrees of Hydrophobicity. *Appl. Catal. A* **2005**, *283*, 225–233.
54. Lu, J.; Fu, B.; Kung, M.C.; Xiao, G.; Elam, J.W.; Kung, H.H.; Stair, P.C. Coking- and Sintering-Resistant Palladium Catalysts Achieved through Atomic Layer Deposition. *Science* **2012**, *335*, 1205–1208.
55. Forman, A.J.; Park, J.; Tang, W.; Hu, Y.; Stucky, G.D.; McFarland, E.W. Silica-Encapsulated Pd Nanoparticles as a Regenerable and Sintering-Resistant Catalyst. *ChemCatChem* **2010**, *2*, 1318–1324.
56. Adijanto, L.; Bennett, D.A.; Chen, C.; Yu, A.S.; Cargnello, M.; Fornasiero, P.; Gorte, R.J.; Vohs, J.M. Exceptional Thermal Stability of Pd@CeO_2 Core-Shell Catalyst Nanostructures Grafted Onto an Oxide Surface. *Nano Lett.* **2013**, *13*, 2252–2257.
57. Schwartz, W.R.; Pfefferle, L.D. Combustion of Methane over Palladium-Based Catalysts: Support Interactions. *J. Phys. Chem. C* **2012**, *116*, 8571–8578.
58. Gannouni, A.; Albela, B.; Zina, M.S.; Bonneviot, L. Metal Dispersion, Accessibility and Catalytic Activity in Methane Oxidation of Mesoporous Templated Aluminosilica Supported Palladium. *Appl. Catal. A* **2013**, *464–465*, 116–127.
59. Zhu, G.; Fujimoto, K.; Zemlyanov, D.Y.; Datye, A.K.; Ribeiro, F.H. Coverage of Palladium by Silicon Oxide during Reduction in H_2 and Complete Oxidation of Methane. *J. Catal.* **2004**, *225*, 170–178.
60. Jacobson, N.S.; Opila, E.J.; Myers, D.L.; Copland, E.H. Thermodynamics of Gas Phase Species in the Si–O–H System. *J. Chem. Thermodyn.* **2005**, *37*, 1130–1137.
61. Opila, E.; Jacobson, N.; Myers, D.; Copland, E. Predicting Oxide Stability in High-Temperature Water Vapor. *JOM* **2006**, *58*, 22–28.

62. Lund, C.R.F.; Dumesic, J.A. Strong Oxide-Oxide Interactions in Silica-Supported Fe_3O_4: III. Water-Induced Migration of Silica on Geometrically Designed Catalysts. *J. Catal.* **1981**, *72*, 21–30.
63. Yoshida, H.; Nakajima, T.; Yazawa, Y.; Hattori, T. Support Effect on Methane Combustion over Palladium Catalysts. *Appl. Catal. B* **2007**, *71*, 70–79.
64. Persson, K.; Ersson, A.; Colussi, S.; Trovarelli, A.; Järås, S.G. Catalytic Combustion of Methane over Bimetallic Pd–Pt Catalysts: The Influence of Support Materials. *Appl. Catal. B* **2006**, *66*, 175–185.
65. Guerrero, S.; Araya, P.; Wolf, E.E. Methane Oxidation on Pd Supported on High Area Zirconia Catalysts. *Appl. Catal. A* **2006**, *298*, 243–253.
66. Card, R.J.; Schmitt, J.L.; Simpson, J.M. Palladium-Carbon Hydrogenolysis Catalysts: The Effect of Preparation Variables on Catalytic Activity. *J. Catal.* **1983**, *79*, 13–20.
67. Kan, H.H.; Colmyer, R.J.; Asthagiri, A.; Weaver, J.F. Adsorption of Water on a PdO(101) Thin Film: Evidence of an Adsorbed HO-H_2O Complex. *J. Phys. Chem. C* **2009**, *113*, 1495–1506.
68. Fujimoto, K.; Ribeiro, F.H.; Avalos-Borja, M.; Iglesia, E. Structure and Reactivity of PdO*x*/ZrO_2 Catalysts for Methane Oxidation at Low Temperatures. *J. Catal.* **1998**, *179*, 431–442.
69. Chin, Y.; Iglesia, E. Elementary Steps the Role of Chemisorbed Oxygen, and the Effects of Cluster Size in Catalytic CH_4-O_2 Reactions on Palladium. *J. Phys. Chem. C* **2011**, *115*, 17845–17855.
70. Ciuparu, D.; Pfefferle, L. Contributions of Lattice Oxygen to the overall Oxygen Balance during Methane Combustion over PdO-Based Catalysts. *Catal. Today* **2002**, *77*, 167–179.
71. Abbasi, R.; Wu, L.; Wanke, S.E.; Hayes, R.E. Kinetics of Methane Combustion over Pt and Pt–Pd Catalysts. *Chem. Eng. Res. Des.* **2012**, *90*, 1930–1942.
72. Yamamoto, H.; Uchida, H. Oxidation of Methane over Pt and Pd Supported on Alumina in Lean-Burn Natural-Gas Engine Exhaust. *Catal. Today* **1998**, *45*, 147–151.
73. Persson, K.; Ersson, A.; Jansson, K.; Iverlund, N.; Järås, S. Influence of Co-Metals on Bimetallic Palladium Catalysts for Methane Combustion. *J. Catal.* **2005**, *231*, 139–150.
74. Persson, K.; Ersson, A.; Jansson, K.; Fierro, J.L.G.; Järås, S.G. Influence of Molar Ratio on Pd–Pt Catalysts for Methane Combustion. *J. Catal.* **2006**, *243*, 14–24.
75. Persson, K.; Jansson, K.; Järås, S.G. Characterisation and Microstructure of Pd and Bimetallic Pd–Pt Catalysts during Methane Oxidation. *J. Catal.* **2007**, *245*, 401–414.
76. Kuper, W.J.; Blaauw, M.; Berg, F.V.; Graaf, G.H. Catalytic Combustion Concept for Gas Turbines. *Catal. Today* **1999**, *47*, 377–389.
77. Ozawa, Y.; Tochihara, Y.; Watanabe, A.; Nagai, M.; Omi, S. Deactivation of Pt·PdO/Al_2O_3 in Catalytic Combustion of Methane. *Appl. Catal. A* **2004**, *259*, 1–7.
78. Ishihara, T. Effects of Additives on the Activity of Palladium Catalysts for Methane Combustion. *Chem. Lett.* **1993**, *22*, 407–410.
79. Carstens, J.N.; Su, S.C.; Bell, A.T. Factors Affecting the Catalytic Activity of Pd/ZrO_2 for the Combustion of Methane. *J. Catal.* **1998**, *176*, 136.
80. Zhu, G.; Han, J.; Zemlyanov, D.Y.; Ribeiro, F.H. The Turnover Rate for the Catalytic Combustion of Methane over Palladium is Not Sensitive to the Structure of the Catalyst. *J. Am. Chem. Soc.* **2004**, *126*, 9896–9897.

81. Monteiro, R.S.; Zemlyanov, D.; Storey, J.M.; Ribeiro, F.H. Turnover Rate and Reaction Orders for the Complete Oxidation of Methane on a Palladium Foil in Excess Dioxygen. *J. Catal.* **2001**, *199*, 291–301.
82. Ribeiro, F.H.; Chow, M.; Dallabetta, R.A. Kinetics of the Complete Oxidation of Methane over Supported Palladium Catalysts. *J. Catal.* **1994**, *146*, 537–544.
83. Hurtado, P.; Ordóñez, S.; Sastre, H.; Díez, F.V. Development of a Kinetic Model for the Oxidation of Methane over Pd/Al_2O_3 at Dry and Wet Conditions. *Appl. Catal. B* **2004**, *51*, 229–238.